Journal Pre-proof

Design, synthesis and biological evaluation of rasagiline-clorgyline hybrids as novel dual inhibitors of monoamine oxidase-B and amyloid-β aggregation against Alzheimer's disease

Sai-Sai Xie, Jing Liu, Chunli Tang, Chengyun Pang, Qing Li, Yuelian Qin, Xiaojie Nong, Zhipeng Zhang, Jie Guo, Maojun Cheng, Weizhong Tang, Ningsheng Liang, Neng Jiang

PII: S0223-5234(20)30446-3

DOI: https://doi.org/10.1016/j.ejmech.2020.112475

Reference: EJMECH 112475

To appear in: *European Journal of Medicinal Chemistry*

Received Date: 28 January 2020

Revised Date: 13 April 2020

Accepted Date: 15 May 2020

Please cite this article as: S.-S. Xie, J. Liu, C. Tang, C. Pang, Q. Li, Y. Qin, X. Nong, Z. Zhang, J. Guo, M. Cheng, W. Tang, N. Liang, N. Jiang, Design, synthesis and biological evaluation of rasagiline-clorgyline hybrids as novel dual inhibitors of monoamine oxidase-B and amyloid-β aggregation against Alzheimer's disease, *European Journal of Medicinal Chemistry* (2020), doi: https://doi.org/10.1016/j.ejmech.2020.112475.

Graphical Abstract

Design, synthesis and biological evaluation of rasagiline-clorgyline hybrids as novel dual inhibitors of monoamine oxidase-B and amyloid-β aggregation against Alzheimer's disease

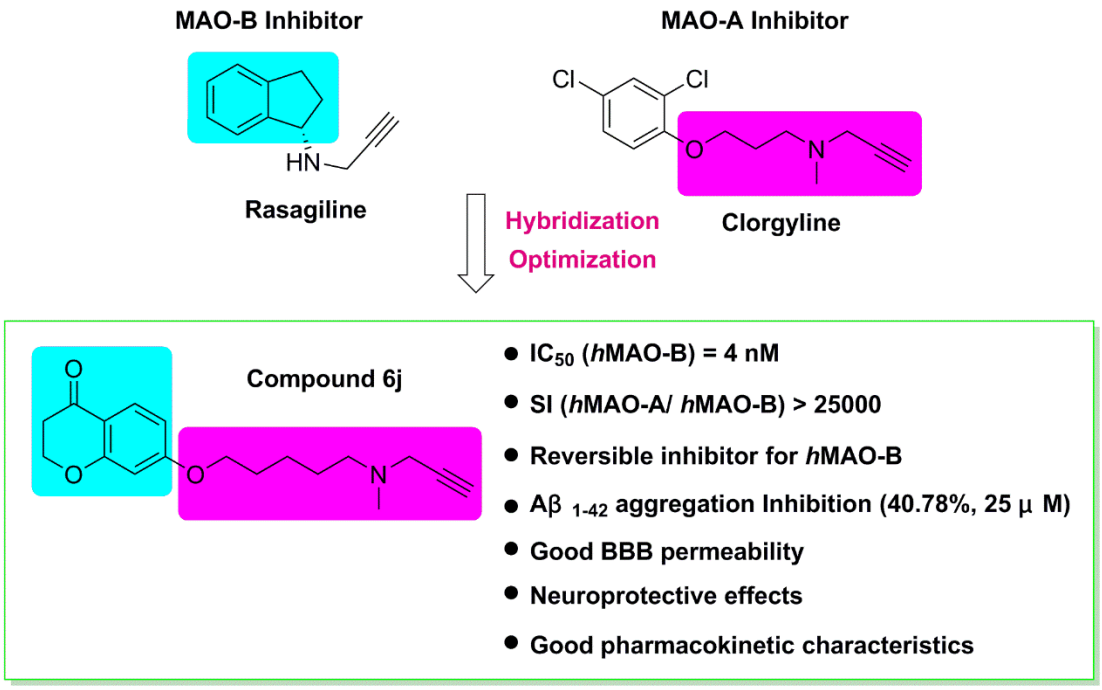

Design, synthesis and biological evaluation of rasagiline-clorgyline hybrids as novel dual inhibitors of monoamine oxidase-B and amyloid-β aggregation against Alzheimer's disease

Sai-Sai Xie[#a,c], Jing Liu[#a,d], Chunli Tang[a], Chengyun Pang[a], Qing Li[a], Yuelian Qin[a], Xiaojie Nong[a], Zhipeng Zhang[c], Jie Guo[c], Maojun Cheng[c], Weizhong Tang[b], Ningsheng Liang[a,*], Neng Jiang[a,*]

[a]Department of Pharmacy, [b]Department of Gastrointestinal Surgery, Affiated Tumor Hospital of Guangxi Medical University, Nanning, PR China

[c]National Pharmaceutical Engineering Center for Solid Preparation in Chinese Herbal Medicine, [d]School of Pharmacy, Jiangxi University of Traditional Chinese Medicine, Nanchang, PR China

*Corresponding authors.

E-mail addresses: Liangn01@163.com (N. Liang), cpujnh@163.com (N. Jiang)

[#]These authors contributed equally to this work.

Abstract

A series of rasagiline-clorgyline hybrids was designed, synthesized and investigated in vitro for their inhibition of monoamine oxidase and amyloid-β aggregation. Most of compounds were found to be selective and highly potent hMAO-B inhibitors showing IC_{50} values in the nanomolar, and exhibited a moderate inhibition of amyloid-β aggregation. 7-((5-(methyl(prop-2-yn-1-yl)amino) pentyl)oxy)chroman-4-one (**6j**) was the most interesting compound identified in this research, endowed with higher hMAO-B potency (IC_{50} = 4 nM) and selectivity (SI>25000) compared to the reference selective inhibitor rasagiline (IC_{50} = 141 nM, SI>355), and exhibited good inhibitory activity against $A\beta_{1-42}$ aggregation (40.78%, 25 μM). Kinetic and molecular modeling studies revealed that **6j** was a competitive reversible inhibitor for hMAO-B. Moreover, compound **6j** displayed low toxicity and good neuroprotective effects in SH-SY5Y cell assay, and could penetrate the blood-brain barrier according to the parallel artificial membrane permeability assay. Pharmacokinetics assay revealed that compound **6j** possessed good pharmacokinetic profiles after intravenous and oral administrations. Overall, these results highlighted that compound **6j** was an effective and promising multitarget agent against Alzheimer's disease.

1. Introduction

Given social development, better living conditions and medical advances, the proportion and lifespan of older people in the global population are increasing. The aging population is a feature trends in developed and developing countries. The aging population is closely related to the increasing incidence rate of neurodegenerative diseases in old age and increasing government expenditure on health and social care. Now the care costs of 35 million patients with dementia was over $ 600 billion per year that is about one percent of global Gross Domestic Product [1]. Kuca et al. [2] simulated prolonging the length of a person's 'stay' in the Mild, Moderate, or Severe stage, the total cost of care for all persons with dementia will increase by 2080. Kuca et al. showed that prolonging the stay in the Mild stage of AD (by lowering the incidence by 10%, 30%, or 50%) reduced the cost (by 4.88%, 16.78% and 32.48%, respectively). Therefore, it is of great significance to develop drugs for the mild and moderate stages of AD.

Alzheimer's disease (AD) is a complex neurodegenerative disease and widely researched owing to the poor efficiency of AD treatment and brain functional damage for daily life inabilities, leading to high familial and social burden for patient care [3, 4]. Alzheimer's Association has reported that there are about 47 million AD patients worldwide, and the number will rise to 100 million by 2050 [5]. Many AD studies have shown that the loss of neurons associated with the aggregation of amyloid-β peptide (Aβ) and hyperphosphorylation of tau protein in the brain regions [6]. Aβ aggregation in neuronal plaques, oxidative stress produced by neuro transmitters and many other factors are mainly causing neuronal degeneration in AD [7, 8]. A multitarget-directed-ligand (MTDL) strategy is more promising and effective for the treatment of AD because of the complex and multifactorial pathological mechanism of AD [9,10].

Monoamine oxidases (MAOs) are flavin adenine dinucleotide (FAD)-containing enzymes that catalyse the oxidative deamination of various biogenic and xenobiotic monoamines such as serotonin, epinephrine, dopamine and xenobiotic amines from dietary [11]. Monoamine oxidases (MAOs) are separated into two different

isoenzymes, namely MAO-A and MAO-B [12, 13]. The two isoform enzymes encoded by different genes exhibit distinct tissue distribution, different substrate and specific inhibition [14-18]. MAO-A is responsible for the oxidative deamination of various neurotransmitters including norepinephrine, serotonin and epinephrine. Clorgyline is an irreversible inhibitor of selective MAO-A, and moclobemide is a reversible inhibitor of selective MAO-A [11]. MAO-B preferentially catalyses the derivative of benzylamine or 2-phenethylamine. Selegiline and rasagiline are selective and reversible inhibitors of MAO-B. MAO-A are associated with depression, whereas MAO-B are used for the treatment of Alzheimer's disease by more and more evidence [19-21]. With increasing age, more and more expression level of MAO-B is found in the patients' brain tissue and cerebral spinal fluid (CSF) [22]. High expression of MAO-B can cause the increment of oxidative free radicals, the disorder of cholinergic neurons and the formation of amyloid plaques [23]. Thus, high selective and reversible inhibitors of MAO-B are considered as promising candidates for AD treatment.

Aβ plaques plays an important role in the key pathological feature of AD. Aβ plaques are mainly consisted of aggregation of Aβ peptide, a 39 to 43 residue long protein degraded from the amyloid precursor protein (APP) [24-25]. Aβ in the brain leads to the formation of oligomers, fibrils and plaques, causing neuronal toxicity, neuronal loss and dementia [26-27]. Therefore, inhibition of Aβ aggregation is also a promising and potential therapy for AD.

Alzheimer's disease is a complex multifactorial neurodegenerative disease, the initiation and progression involve multiple targets or factors [28]. The approach "one molecule, one target" does not always lead to satisfactory efficacy. Two approaches are often used for multi-target therapeutics. The first approach is combinations of drugs with one target or a single active ingredient respectively, whereas the second approach is multi-target directed ligands (MTDLs) [29]. The former approach has some advantages, such as providing better dose flexibility by directly adjust ratio of drugs in mixture, lower treatment cost. However, combinations of drugs often suffered from more adverse effects such as dose-limiting toxicities, drug-drug

interactions, complex PK/PD properties of the multiple components and poor patient compliance [30-31]. MTDLs that are new chemical entity have some advantages, such as the PK/PD properties be easier to formulate compared with a mixture, the increasing therapeutic efficacy through synergies at low dosages and reduced adverse effects enable wider therapeutic windows [32-34]. Sun [35] et al. had discussed the advantages and disadvantages of the above two approaches.

Our group have made great efforts to find potential multitarget-directed-ligands (MTDLs) targeting monoamine oxidases, cholinesterase, Aβ protein and oxidative free radicals etc [36-39]. In this paper, a series of rasagiline-clorgyline hybrids was designed, synthesized and evaluated for their biological activities, toxicity and pharmacokinetics. In addition, the development of new drugs targeted to the CNS requires good blood brain-barrier (BBB) permeability. A good permeability through the BBB is essential because of the target site of AD is located in the CNS [40-41]. Drugs that can penetrate BBB is a challenging issue in AD therapy. Thus, to evaluate the compounds whether have good brain penetration as early as possible [42-43], a well-known high throughput screening (HTS) technique, parallel artificial membrane permeation assay, was performed. Without consideration of P-glycoprotein (Pgp) efflux, high plasma protein binding and low capillary permeability, this method can quickly predict the ability of present compounds to cross the BBB [40]. Furthermore, kinetic and molecular modeling studies were also performed to investigate the high selective and strong affinity modes of compound **6j** with hMAO-B.

2. Results and discussion

2.1. Design of rasagiline-clorgyline hybrids

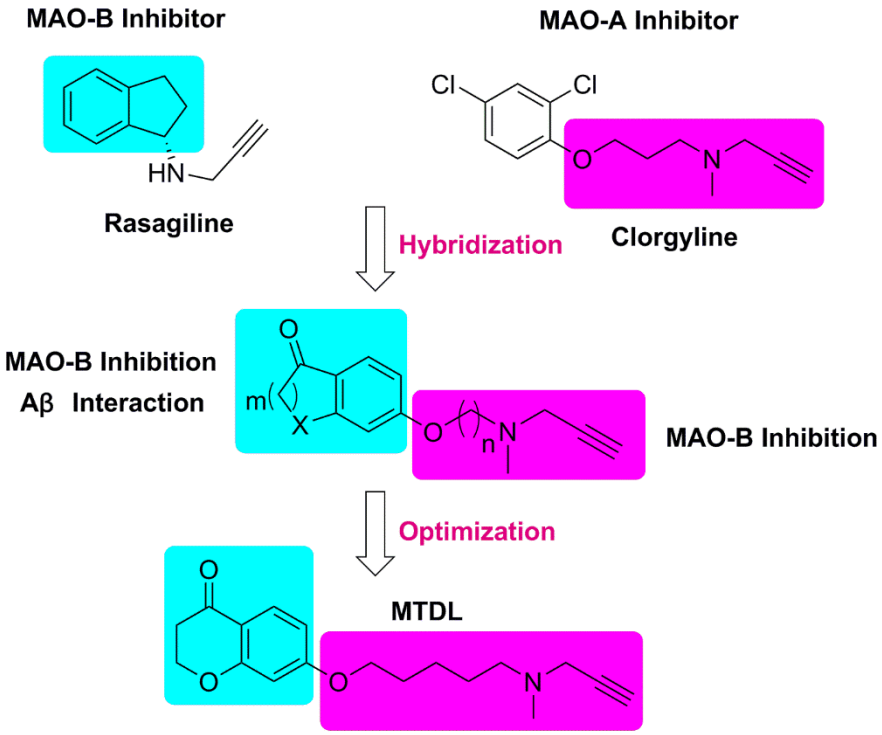

Fig. 1. Design strategy for rasagiline-clorgyline hybrids

Clorgyline (hydrochloride) is an irreversible, potent and selective MAO-A inhibitor with IC_{50} values of 0.0046 μM for MAO-A and 62 μM for MAO-B. Rasagiline is a potent, selective and irreversible monoamine oxidase B (MAO-B) inhibitor. As shown in **Fig.1**, the 2,3-dihydro-1*H*-indene analogues of rasagiline show the inhibitory activity for amyloid-β aggregation. Given the similar structure between clorgyline and rasagiline, the drug fragment of clorgyline and rasagiline are combined to design and optimize a series of rasagiline-clorgyline hybrids, which are expected to be highly selective and potent hMAO-B inhibitors, as well as Aβ aggregation inhibitors. In addition, we focus the structural optimization of 2,3-dihydro-1*H*-indene (marked at the blue color as shown in **Fig.1.**) and the length of flexible linker (marked at the red color as shown in **Fig.1.**). Rasagiline-clorgyline hybrids and its analogues are under investigation for the treatment of Alzheimer's disease.

2.2. Chemistry

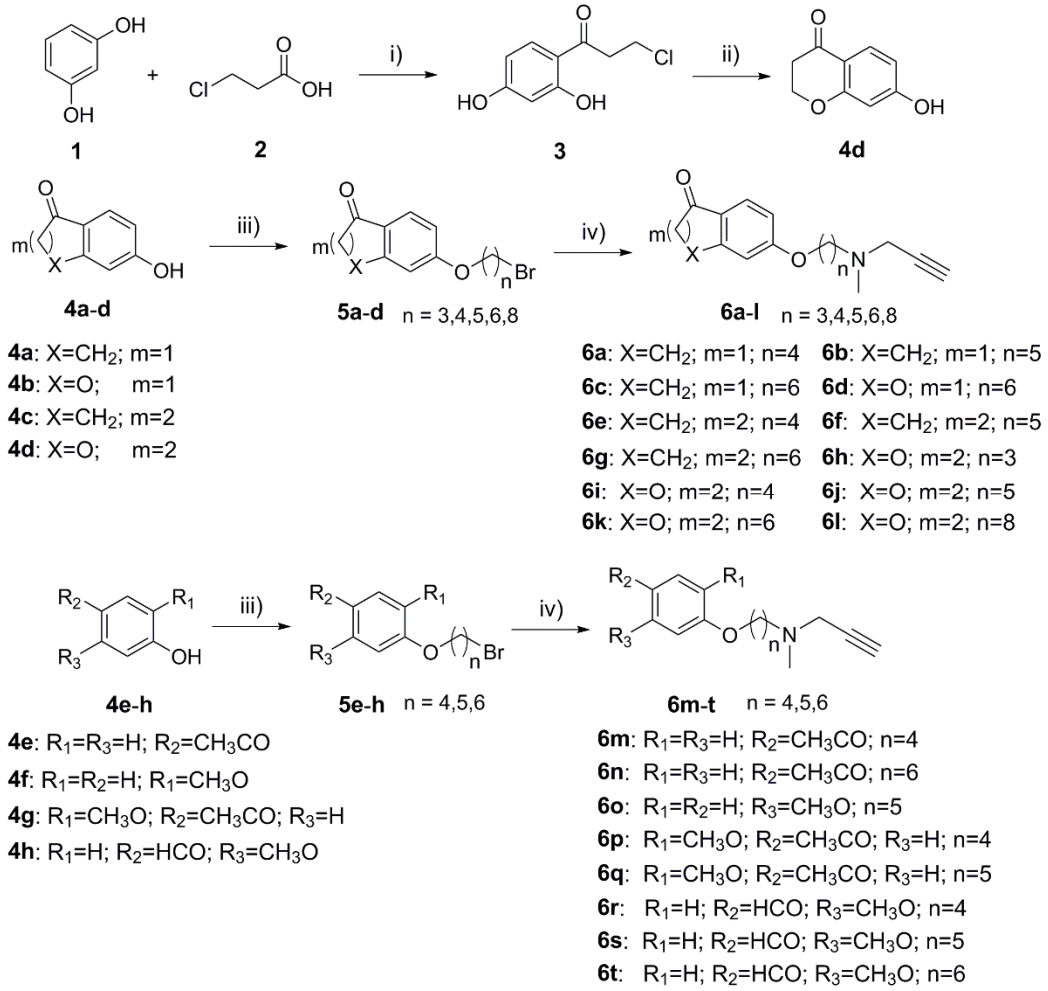

Scheme 1. Synthesis of rasagiline-clorgyline hybrids **6a-6t**. Reagents and conditions: (i) CF_3SO_3H, 80 °C, 30 min; (ii) 2 M NaOH (aq), 5 °C to r.t., 6 M H_2SO_4 (aq), 2 h; (iii) α, ω-dibromoalkanes, K_2CO_3, DMF, reflx, 4 h; (iv) propargyl amine, anhydrous K_2CO_3, KI, CH_3CN, 65 °C, 1-2 h.

The target compounds were synthesized as shown in **Scheme 1**. The initial compound **4a-4c** and **4e-4h** were purchased from the market. The initial compound **4d** was obtained according to our previously reported experimental method [42]. The alkylation of compound **4a-4h** with corresponding α, ω-dibromoalkanes under K_2CO_3 alkaline condition at 70 ^oC generated products **5a-h**. It was noted that the reactivity equivalent of corresponding α, ω-dibromoalkanes were ranged from 4 to 6. Finally, the target compounds **6a-6t** were obtained by nucleophilic substitution of compounds **5a-h** with the appropriate propargylamine in the presence of K_2CO_3 and DMF at 60 ^oC.

*2.3.MAOs inhibitory activities of all synthesized compounds **6a-6t**.*

The *h*MAO-A and *h*MAO-B inhibitory potencies of compounds **6a-6t** were tested by a reported fluorescence-based Amplex Red assay using clorgyline, rasagiline and iproniazid as reference compounds [44]. The *h*MAO inhibition IC_{50} values and corresponding selectivity indexes (SI = IC_{50} MAO-A/IC_{50} MAO-B) obtained for all synthesized compounds **6a-6t** and reference compounds were shown in **Table 1**. Most of the design compounds exhibited potent the inhibition of *h*MAO-B enzymatic activity in nanomolar. On the contrary, the same compounds showed no inhibition or poor efficacy against *h*MAO-A, up to the highest concentration tested (100 μM). Owing to the MAO-A inhibition may cause adverse reaction in the peripheral tissues, these high selective and potent inhibitors of MAO-B activity will be more beneficial for AD treatment. Recently, some research groups had reported represented MAO-B inhibitors, such as hydroxypyridinonecoumarin hybrids [45], (Pyrrolo-pyridin-5-yl)benzamides [46], 1-Propargyl-4-Styrylpiperidine-Like Analogues [47], 4H-benzopyran-4-one derivatives [48]. Most of these compounds show similar potent and less selective than compound **6j**.

In the series hybrids **6a-6t**, compound **6j** was the most potent and the highest selective inhibitors of hMAO-B (IC_{50} = 4 nM, SI > 25000), which was more potent and selective than the reference compounds rasagiline and iproniazid (IC_{50} = 141.7 nM and 7410 nM, SI >355 and = 0.89, respectively), as shown in **Table 1**. Due to the linker length between aromatic ring and propargyl amine having relations with the MAOs inhibitory potencies, compounds with the different linker length were synthesized for evaluation of MAOs inhibition activity. A comparison of inhibitory capabilities of the compounds **6h-6l** (n = 3-8) showed that the inhibitory activity for MAO-B was increased with the increase of carton chain length (from 3 carbon atoms to 5 carbon atoms), but decreased with further longer carton chain (from 5 carbon atoms to 8

Table 1. MAOs inhibitory activities of rasagiline-clorgyline hybrids **6a-6t**.

Compound	X	R_1	R_2	R_3	m	n	$IC_{50} \pm$ SD (nM)[a]	SI[c]

							*h*MAO-A	*h*MAO-B	
6a	CH_2	-	-	-	1	4	7.93±1.03% [b]	366.3±13.2	> 273[#]
6b	CH_2	-	-	-	1	5	31.01±4.21% [b]	94.8±5.8	> 1055[#]
6c	CH_2	-	-	-	1	6	4.42±0.97% [b]	128.6±9.1	> 777[#]
6d	O	-	-	-	1	6	11.67±1.03% [b]	51.9±5.7	> 1927[#]
6e	CH_2	-	-	-	2	4	30.88±4.97% [b]	72.5±7.4	> 1379[#]
6f	CH_2	-	-	-	2	5	26.05±2.14% [b]	46.3±3.8	> 2160[#]
6g	CH_2	-	-	-	2	6	24.99±4.50%[b]	133.1±8.5	> 751[#]
6h	O	-	-	-	2	3	32.14±11.32%[b]	11414±128	> 9[#]
6i	O	-	-	-	2	4	22.78±3.26%[b]	58.9±5.7	> 1698[#]
6j	**O**	-	-	-	**2**	**5**	**6.04**±0.74**% [b]**	**4.0±0.6**	**>2.5*10[4] [#]**
6k	O	-	-	-	2	6	34.06±6.25% [b]	117.0±8.3	> 855[#]
6l	O	-	-	-	2	8	28.65±3.68%[b]	422.0±15.2	> 237[#]
6m	-	H	CH_3CO	H	-	4	28.61±4.11% [b]	56.51±4.1	> 1770[#]
6n	-	H	CH_3CO	H	-	6	37.28±5.33% [b]	20.42±2.2	> 4897[#]
6o	-	H	H	CH_3O	-	5	32.33±9.46%[b]	100.86±7.9	> 991[#]
6p	-	CH_3O	CH_3CO	H	-	4	21.10±2.21% [b]	1150±37	> 87[#]
6q	-	CH_3O	CH_3CO	H	-	5	39.52±7.52% [b]	6520±24	> 15[#]
6r	-	H	HCO	CH_3O	-	4	29.37±3.88% [b]	41.25%[b]	-
6s	-	H	HCO	CH_3O	-	5	27.13±10.11% [b]	5735±120	> 17[#]
6t	-	H	HCO	CH_3O	-	6	37.39±7.93% [b]	551.8±33	> 181[#]
Clorgyline							4.58±0.35	62010±870	0.000074
Rasagiline							47.91±2.31%[b]	141.70±6.34	> 355[#]
Iproniazid							6590 ± 270	7410 ± 340	0.89

[a] Data are expressed as mean ± S.D. from three diferent experiments; [b] Inhibition% at 100 μM. [c]SI: hMAO-B selectivity index = IC_{50}(*h*MAO-A)/ IC_{50}(*h*MAO-B). [d] Inhibition% at 50 μM. [#] Values obtained under the assumption that the corresponding IC_{50} against MAO-A was the highest concentration tested (100 μM).

carbon atoms). Compound **6j** (IC_{50} = 4 nM) with a five-carbon chain presented more potent activity than the corresponding compound **6h** containing three-carbon chain

(IC_{50} = 11414 nM) and **6i** containing four-carbon chain (IC_{50} = 58.9 nM). However, the compound **6k** containing six-carbon chain (IC_{50} = 117 nM) and **6l** with eight-carbon atom chain (IC_{50} = 422 nM) showed less inhibitory activity than compound **6j** containing a five-carbon chain (IC_{50} = 4 nM). Similar structure-activity relationships (SARs) were also found in other compounds, such as compounds **6a-6c**, **6e-6g** and **6r-6t**.

After exploring the SARs of chain length, the SARs of different heterocycle were also explored. As shown in **Table 1**, the target compounds containing six-membered heterocycle (**6e**, **6f**) was about 5-fold and 2-fold more potent than the corresponding target compounds (**6a**, **6b**) containing five-membered heterocycle, whereas compounds **6g** containing six-membered heterocycle and compounds **6c** containing five-membered heterocycle showed similar potency. A comparison of the potency of the four rasagiline-clorgyline hybrids (**6d**, **6k**, **6c**, **6g**) revealed that the replacement of carbon atom with oxygen atom substituent at the position 3 of benzene ring (**6d** vs. **6c**, **6k** vs. **6g**) provided more hMAO-B inhibitory activity. Given the above discussion, the chromanone moiety (compound **6k** with IC_{50}: 116 nM) produced an increment in potency when compared to 2,3-dihydro-1*H*-inden-1-one (compound **6c** with IC_{50}: 128.6 nM) and 3,4-dihydronaphthalen-1(2*H*)-one moieties (compound **6g** with IC_{50}: 133.1 nM). Furthermore, the ring-opening of benzofuran-3(2*H*)-one moiety (compound **6d**) was to generate analogues **6r**, **6s** and **6t**. The corresponding functional group of these analogues **6r-6t** were expressed as R_2=HCO- and R_3 = CH_3O- substituents. Surprisingly, the ring-opening analogues **6r-6t** resulted in dramatic reduction in potency towards MAO-B compared to the corresponding heterocycle **6d**. It was worth noting that, the acetyl (R_2 = CH_3CO-) substituent group at the position 4 of benzene ring were necessary for the potent hMAO-B inhibitory activity, as compounds **6m** and **6n** showed significant MAO-B inhibition activity (IC_{50} = 56.51, 20.42 nM, respectively). Finally, the additional substitution with methoxy group (R_1 = CH_3O-) at the position 2 of benzene ring (compounds **6p** and **6q**) exhibited a dramatic loss of *h*MAO-B potency, compared to compounds **6m** and **6n**.

*2.4. Docking studies of compound **6j** with hMAO-B*

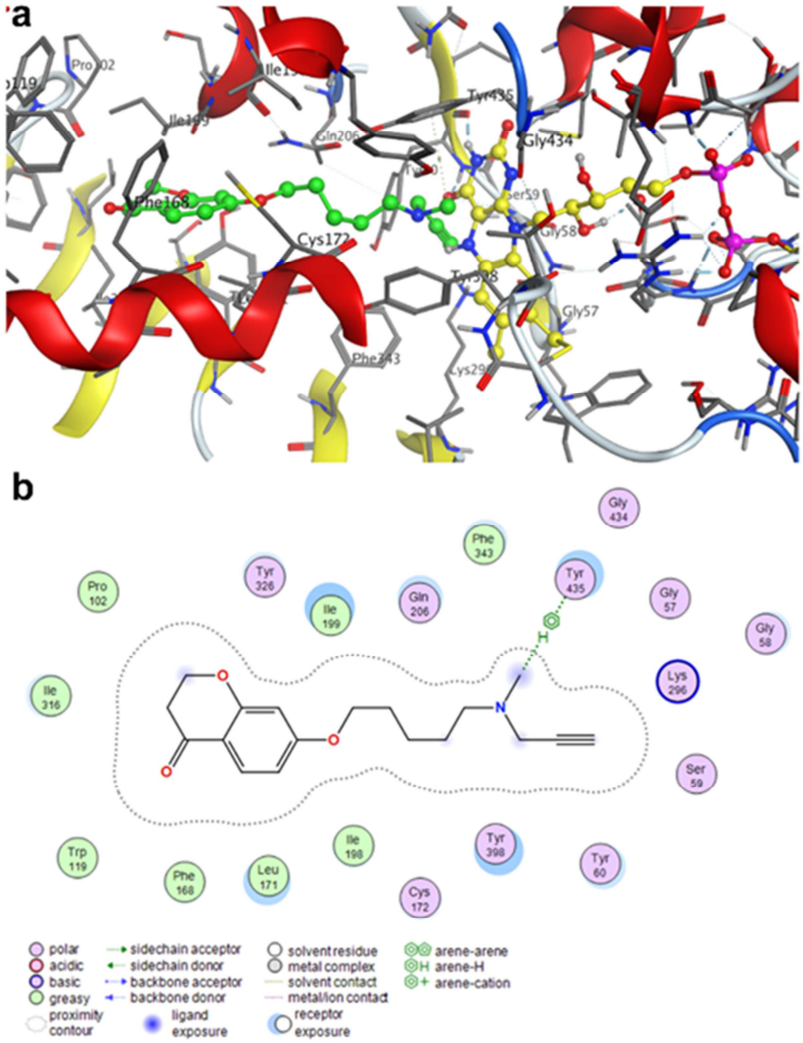

Fig. 2. (a) 3D docking model of compound **6j** with *h*MAO-B. Atom colors: green-carbon atoms of **6j**, gray-carbon atoms of residues of *h*MAO-B, yellow-carbon atoms of FAD, dark blue-nitrogen atoms, red-oxygen atoms. The green dashed line represents the interaction between the protein and the ligand. (b) 2D schematic diagram of docking model of compound **6j** with *h*MAO-B. The figure was prepared using the ligand interactions application in MOE.

In order to rationalize the binding modes of the synthesized compounds with *h*MAOs at molecular level, docking studies were carried out by the Molecular Operating Environment (MOE 2015.10) software. The compound **6j** with highly selective and most potent toward *h*MAO-B was selected and researched its *h*MAO-B binding modes. The binding mode of compound **6j** with respect to MAO-B was investigated based on the X-ray crystal structure of the human monoamine oxidase B in complex with 7-(3-chlorobenzyloxy)-4-(methylamino)methyl-coumarin (PDB code 2V61), and the protein was energy minimized and 3D protonated using the structure

preparation module of MOE. It can be seen from the **Fig. 2.** that the propargylamine moiety of compound **6j** was oriented to the flavin adenine dinucleotide (FAD) cofactor and establish a 'arene-H' interaction with Tyr 435 in the substrate cavity. The chromanone moiety occupied the entrance cavity and interacted with leu171, Cys172, Ile198, Ile199, Ile 316, Tyr 326, Trp 119 and Phe168 through van der waals and hydrophobic interactions. For comparison purpose, rasagiline was also selected for docking studies (Fig **S1**). The results showed that compound **6j** and rasagiline showed very similar docking poses in the substrate cavity of MAO-B; however, in comparison to the rasagiline, compound **6j** could also interact with the residues in entrance cavity of MAO-B, thereby exhibiting higher binding affinity to MAO-B than rasagiline.

2.5. Reversibility and kinetic study of hMAO-B inhibition

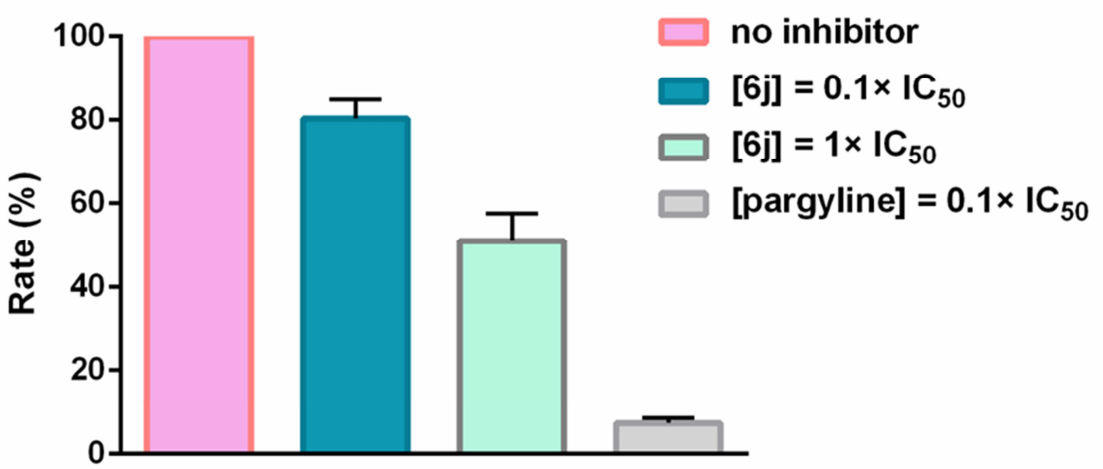

Fig. 3. Recovery of enzyme inhibition activity after dilution of enzyme-compound complex. hMAO-B were pre-incubated with compound **6j** at 10 × IC_{50} concentration and 100 × IC_{50} concentration for 30 min and then diluted to 0.1 × IC_{50} and 1 × IC_{50} concentrations, respectively.

It was well known that reversible inhibitors are more effective for the treatment of AD than irreversible inhibitors. The most promising compound **6j**, a highly selective and potent MAO-B inhibitor, was selected for further studies. A reported enzyme inhibition experiment [49-50] was carried to investigate whether compound **6j** was reversible or irreversible, and pargyline was used as irreversible reference compound. Firstly, the MAO-B enzyme and compound **6j** were incubated together at

concentrations of 0, 10 and 100 × IC_{50} for 30 min, respectively. Then, these 10 and 100×IC_{50} concentrations of enzyme-compound complex were diluted to corresponding concentrations of 0, 0.1 and 1×IC_{50}. The tested compound will be reversible if the activity of the enzyme is restored to about 90% and 50% after dilution to 0.1×IC_{50} and 1×IC_{50}, respectively. The tested compound will be irreversible if the activity of the enzyme is no longer restored after dilution. As shown in **Fig. 3**, the activity of MAO-B enzyme was restored to about 82% and 45% after compound **6j** dilution to 0.1× IC_{50} and 1× IC_{50}, respectively. The activity of MAO-B enzyme was no longer restored (less than 10% of control) after the reference irreversible inhibitor pargyline be diluting. These results showed that compound **6j** is a reversible MAO-B inhibitor.

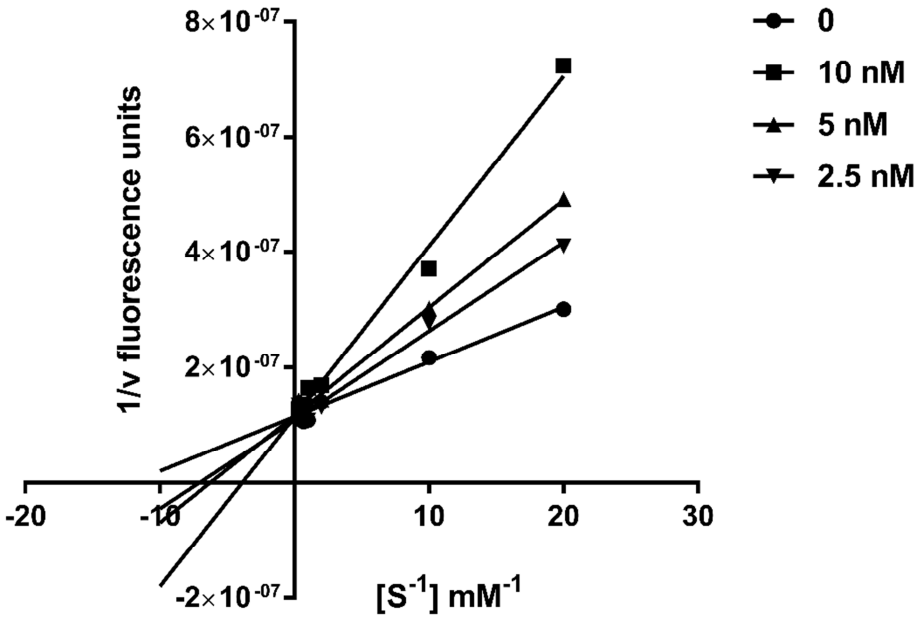

Fig. 4. Kinetic study on the mechanisms of interaction between *h*MAO-B and compound **6j**. Overlaid Lineweaver–Burk reciprocal plots of *h*MAO-B at different concentrations of compound **6j** (2.5, 5 and 10 nM) using *p*-tyramine (0.05–3.0 mM) as substrate.

Furthermore, an enzyme kinetic study on the mechanisms of interaction between *h*MAO-B and compound **6j** was carried out. As shown in **Fig. 4**, the Lineweavere-Burk reciprocal plots were established by rates of MAO-B catalyzed oxidation for *p*-tyramine at different concentrations of compound **6j** (2.5, 5 and 10

nM). All lines were orthogonal on the Y-axis, which suggested that compound **6j** was a competitive MAO-B inhibitor.

*2.6. $A\beta_{1-42}$ self-aggregation inhibitory activity of all synthesized compounds **6a-6t***

All synthesized compounds tested for their MAOs inhibitory activity were also evaluated for their capabilities against $A\beta_{1-42}$ self-induced aggregation by thioflavin-T based fluorescence assay [51-53]. Curcumin (Cur) were used as reference compounds, and $A\beta_{1-42}$ self-aggregation inhibitory activity data of all synthesized compound were summarized in **Table 2**. As can be seen from the **Table 2**, most of compounds showed weak-to-moderate potencies compared to the reference compound curcumin (46.1 ± 6.71%, at 25 μM). Compounds **6i**, **6j** which exhibited remarkable inhibitory activities against MAO-B, had good inhibition property of Aβ self-induce aggregation (43.9 ± 4.85%, 40.78 ± 6.27% at 25 μM). It was hard to draw the structure-activity relationships, due to the vague outline between these compounds and inhibitory activities of Aβ self-aggregation.

Table 2. Inhibitions of $A\beta_{1-42}$ self-induced aggregation of rasagiline-clorgyline hybrids **6a-6t**.

Compound	Inhibition rate (%)[a]	**Compound**	Inhibition rate (%)[a]
6a	31.27 ± 3.01%	**6k**	0.66 ± 0.26%
6b	11.37 ± 1.10%	**6l**	0.34 ± 0.08%
6c	0.68 ± 0.22%	**6m**	6.18 ± 1.97%
6d	9.76 ± 1.53%	**6n**	12.72 ± 2.04%
6e	13.39 ± 1.41%	**6o**	22.23 ± 4.55%
6f	10.28 ± 2.34%	**6p**	21.79 ± 2.74%
6g	18.15 ± 2.17%	**6q**	5.74 ± 0.31%
6h	7.77 ± 2.19%	**6r**	0.86 ± 0.14%
6i	43.9 ± 4.85%	**6s**	0.82 ± 0.20%
6j	40.78 ± 6.27%	**6t**	0.99 ± 0.33%
Curcumin	46.1 ± 6.71%		

[a] Inhibition of self-induced $A\beta_{1-42}$ aggregation (means ± SD of three experiments). The thioflavin-T fluorescence method was used, and the measurements were carried out in the presence of 25 μM inhibitor.

To further analyze the effect of compounds on inhibition of Aβ aggregation, compound **6j** with potent inhibitory activity was selected for the TEM assay. The results indicated that the TEM image analysis is consistent with ThT binding assay (**Fig S2 and S3**). More well-defined $A\beta_{1-42}$ aggregates were observed in the presence of Aβ alone, and fewer $A\beta_{1-42}$ aggregates were observed when compound **6j** and curcumin were added to the samples.

2.7. In vitro blood-brain barrier permeation assay

The blood-brain barrier (BBB) was the main obstacle of the entrance of the anti-AD agents for central nerval system into the brain. Hence, it was necessary to assess the blood-brain barrier permeability of target compounds. The blood-brain barrier

Table 3. Permeability P_e ($\times 10^{-6}$) in the PAMPA-BBB assay for 9 commercial drugs in the experiment validation.

Commercial drugs	Bibliography[a]	Experiment[b]
Testosterone	17.0	16.06 ± 0.53
Estradiol	12.0	12.45 ± 0.46
Progesterone	9.3	9.26 ± 0.34
Chlorpromazine	6.5	7.12 ± 0.17
Corticosterone	5.1	2.17 ± 0.08
Hydrocortisone	1.9	0.76 ± 0.02
Caffeine	1.3	1.54 ± 0.05
Atenolol	1.02	1.66 ± 0.11
Theophylline	0.1	0.69 ± 0.03

[a] Taken from Ref [54].

[b] Experimental data are expressed as mean ± SD from three independent experiments, using PBS : EtOH (70:30) as solvent.

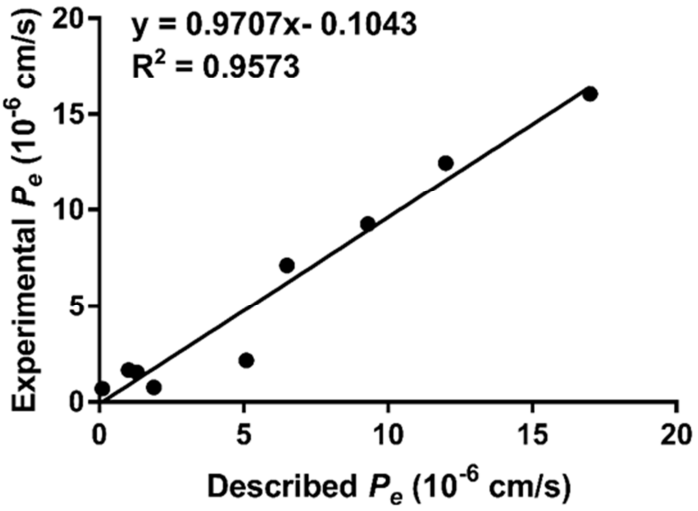

Fig. 5. Lineal correlation between experimental and reported permeability of commercial drugs using the PAMPA-BBB assay. P_e (exp.) = 0.9707 P_e (bibl.) - 0.1043 (R_2 = 0.9573).

Table 4. Permeability P_e ($\times 10^6$ cm/s) in the PAMPA-BBB assay for the target compounds and their predicted penetration into CNS.

Compound	P_e ($\times 10^6$ cm/s)[a]	Prediction[b]
6a	9.61 ± 0.88	CNS^+
6b	10.91 ± 1.02	CNS^+
6c	12.85 ± 0.91	CNS^+
6d	8.30 ± 0.54	CNS^+
6e	8.70 ± 0.65	CNS^+
6f	10.63 ± 0.73	CNS^+
6g	8.58 ± 0.43	CNS^+
6h	9.21 ± 0.32	CNS^+
6i	13.66 ± 1.01	CNS^+
6j	10.25 ± 0.68	CNS^+
6k	8.54 ± 0.42	CNS^+
6l	8.91 ± 0.61	CNS^+
6m	10.63 ± 0.40	CNS^+
6n	8.69 ± 0.52	CNS^+
6o	10.54 ± 0.39	CNS^+

6p	12.53 ± 0.87	CNS^+
6q	12.94 ± 0.94	CNS^+
6r	13.14 ± 1.12	CNS^+
6s	14.04 ± 0.64	CNS^+
6t	11.18 ± 0.39	CNS^+

[a] Permeability P_e ($\times 10^6$ cm/s) values were expressed as mean±SD from three independent experiments, using PBS: EtOH (70:30) as solvent.

[b] CNS^+ was predicted as high BBB permeation with P_e ($\times 10^6$ cm/s) > 3.78.

(BBB) was detected by the parallel artificial membrane permeation assay [54]. As shown in **Table 3**, 9 commercial drugs endowed with reported values were used as reference compounds. Described P_e were regarded as dependent variables and experimental P_e as independent variables when we performed simple linear regression analysis: P_e (exp.) = 0.9707 P_e (bibl.) - 0.1043 (R_2 = 0.9573) (**Fig. 5**). Based on this equation and the limit established by Di et al. for BBB permeation, the value of permeability was as follow: P_e ($\times 10^6$ cm/s) > 3.78 represented high BBB permeation (CNS^+). From **Table 4**, the P_e values of all compounds were higher than 3.78, which indicated all compounds had high permeability of blood-brain barrier.

2.8. SH-SY5Y neuroblastoma cell toxicity

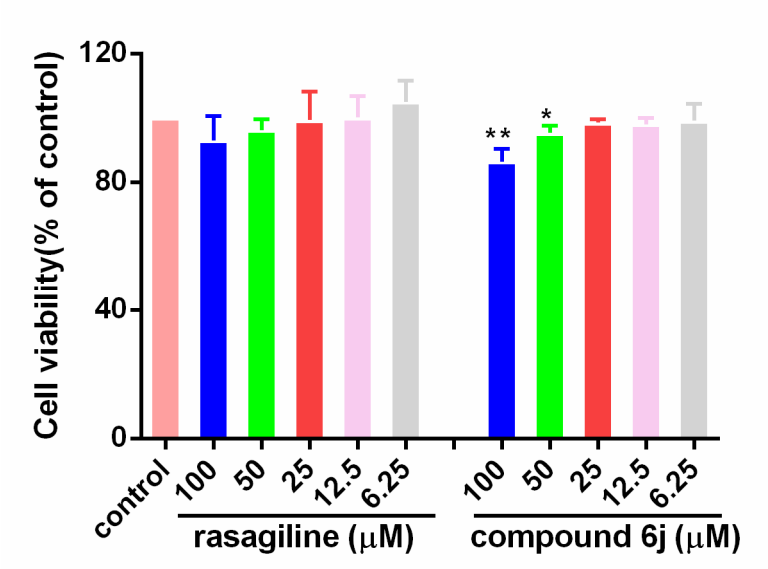

Fig. 6. SH-SY5Y cell viability after treatment of various concentrations of compound **6j** by MTT assay. Data were shown as mean ± SD of three independent experiments (*P <0.05, **P <0.01, compared to control group).

To evaluate the biological safety of these potent inhibitors for MAO-B and amyloid-β aggregation, compound **6j** was selected for cytotoxicity test in human neuroblastoma cell line (SH-SY5Y). SH-SY5Y cells were incubated with different concentrations of compound **6j** for 24h, and then the cell viability was tested by the 3-(4,5-dimethylthiazol-2-yl)-2,5-diphenyltetrazolium (MTT) experiment [55]. As shown in **Fig. 6**, compound **6j** showed non-toxic at the concentrations of 25 μM. Due to the high inhibitory potency of compound **6j** on MAO-B, it would be safe at therapeutic concentration.

2.9. Neuroprotection assays in SH-SY5Y cells

The neuroprotection was extraordinary significant for AD treatment, so the potential protective effects against neurotoxins-induced damage was investigated in SH-SY5Y cells using the method described by zheng et al [56]. Compound **6j** was selected to

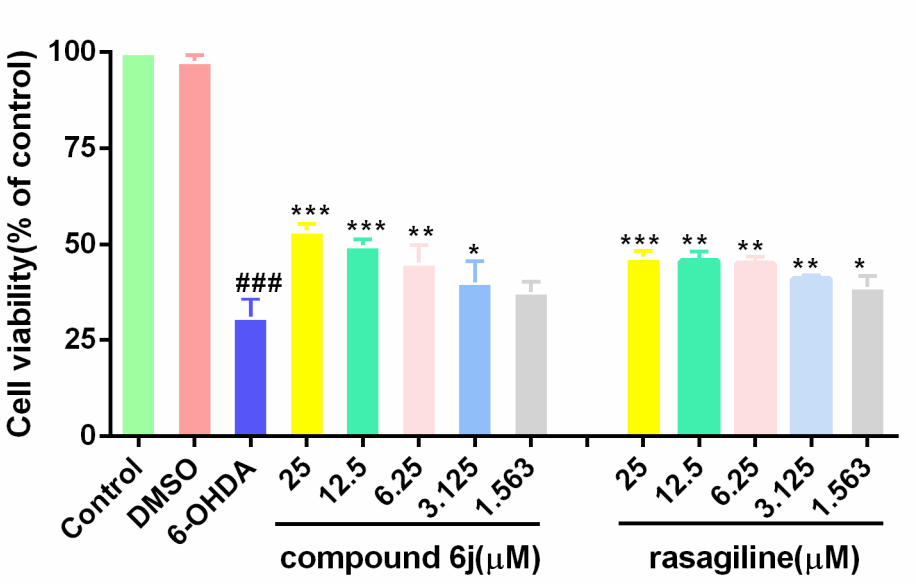

Fig. 7. Neuroprotective effects of compound **6j** against 6-OHDA-induced toxicity in SH-SY5Y cells. Rasagiline was the reference compound. Results were shown as cell viability. All data were the means ± SEM of three independent experiments (*P <0.05, **P <0.01, ***P <0.01, compared to 6-OHDA group).

verify the neuroprotective effect. The bar chart of **Fig. 7** showed that cell viability rate of 6-hydroxydopamine-treated SH-SY5Y cell group significantly decreased when compared to that of control and DMSO group. Different concentrations of compound

6j were respectively incubated with 6-OHDA (200 μM) in SH-SY5Y cells for 24h, and the corresponding cell viability rates were tested by MTT assay. Cell survival rates were gradually increased when 6-OHDA-treated SH-SY5Y cells were respectively incubated with 1.563, 3.125, 6.25, 12.5, 25 μM (the increasing concentrations) of compound **6j**. A similar phenomenon of reference compound rasagiline was also observed under the same conditions. The results indicated that compound **6j** had neuroprotective capability against neurodegeneration disease.

*2.10. Pharmacokinetic evaluation of compound **6j***

Compound **6j** with potent inhibitory activities for MAO-B and $A\beta_{1-42}$ self-aggregation was selected as representatives for further pharmacokinetic studies following intravenous (iv) and oral (po) dosing in SD rats. The key pharmacokinetic parameters of compound **6j** were shown in **Table 5**. Compound **6j** showed a high maximal concentration (C_{max} = 639.29 and 142.17 μg/L), appropriate half-life ($t_{1/2}$ = 1.02 and 1.33 h), and good oral bioavailability (36.1%). These results suggested that compound **6j** would have acceptable pharmacokinetic properties.

Table 5. Pharmacokinetic parameters of compound 6j after po and i.v. administration

Parameters [a]	$T_{1/2}$ (h)	T_{max}(h)	C_{max}(μg/L)	AUC_{0-inf} (μg/L*h)	Cl(L/h/kg)	F%
i.v. (3 mg/kg)	1.02±0.17	-	639.29±89.06	247.74±11.48	3.33±0.15	-
po (10 mg/kg)	1.33±0.16	0.3	142.17±72.21	268.49±69.72	-	36.10%

[a] Compounds were dosed to equal number of male Sprague-Dawley rats in po (10 mg/kg) and i.v. (3 mg/kg) administration (n = 3).

3. Conclusion

To seek effective drugs for Alzheimer disease, a series of new dual inhibitors **6a-6t** by hybridization of rasagiline and clorgyline were designed, synthesized and evaluated. All the target compounds were investigated for their ability to inhibit the monoamine oxidases and amyloid-β aggregation. We were surprised to find that all compounds were selective hMAO-B inhibitors with IC_{50} values ranging from 5.7 μM to 4 nM, and could penetrate the blood-brain barrier. Among these compounds, compound **6j** exhibited higher *h*MAO-B potency and selectivity (IC_{50} = 4 nM, SI>25000) than the reference inhibitor rasagiline (IC_{50}=141 nM, SI > 355), as well as

good inhibition of $A\beta_{1-42}$ aggregation. In addition, kinetic and molecular modeling studies suggested compound **6j** was a competitive and reversible inhibitor for *h*MAO-B. Meanwhile, compound **6j** showed low cytotoxicity and neuroprotective effects according to cell viability and neuroprotection activity assay. The further pharmacokinetics studies showed that compound **6j** had good pharmacokinetic characteristics after intravenous and oral administrations. These properties highlighted that compound **6j** could serve as an effective and promising candidate for AD therapy.

4. Experimental section

4.1. Chemistry

Chemicals were purchased from Sinopharm Chemical Reagent Co., Ltd. (China). Thin layer chromatography (TLC, GF254 Qingdao Haiyang Chemical, QingDao, China) was used for checking reaction, and components were visualized using UV light. The compounds were purified by column chromatography (silica gel, 90-150 mm; Qingdao Marine Chemical Inc.). The synthesized compounds were characterized by melting points apparatus, ^{1}H NMR, ^{13}C NMR and a Mariner ESI-TOF spectrometer (HRESIMS) respectively. ^{1}H NMR and ^{13}C NMR spectra were recorded on a Bruker AM-600 spectrometer, using $CDCl_3$ or DMSO-d_6 as the solvent.

*4.2. 3-Chloro-1-(2,4-dihydroxyphenyl)propan-1-one (**3**)*

A mixture of resorcinol (5.5 g) and 3-chloropropionic acid (5.4 g) were added triflormethanesulfonic acid (15 g). The reaction was stirred at 80 ^{o}C for 30 min. The completed reaction solution was cool to room temperature and then poured into ice water (120 ml). The water solution was extracted with Cl_2CH_2. The Cl_2CH_2 layer was concentrated under vacuum to afford crude product used for the next reaction, without further purification. It is the same method as our group reported reference [42].

*4.3. 7-Hydroxychroman-4-one (**4d**)*

To a solution of 2 N aqueous, crude compound 3 was added and stirred at room temperature for 2h. After the reaction completed, the solution was acidified with 6 M H_2SO_4 to PH = 2, and then was extracted with ethyl acetate. The product **4d** was purified by silica gel chromatography. Structural identification data of compound **4d** as shown in our reported reference [42].

*4.4. General procedures for the preparation of compounds **6a-6t***

A mixture of compound **4a-4h** (4 mmol), suitable α, ω-dibromoalkanes (40 mmol) and powdered K_2CO_3 (8 mmol) in acetone was stirred at reflux for 4h. The obtained residue was purified by silica gel chromatography with PE/EA (6:1) as elution solvent to give compounds **5a-h** [42]. To a solution of compounds **5a-5h** (1 mmol) and K_2CO_3 (2 mmol) in DMF was added propargyl amine (1.4 mmol). The reaction was stirred at 60 ^oC for 6-12 h. After completion, the residue was added ethyl acetate, and the organic phase was washed with water three times. The combined organic phase, dried over anhydrous Na_2SO_4, concentrated on vacuum, and was purified by silica gel chromatography with PE/EA (4:1) as eluent to obtain the target compounds **6a-6t**.

*4.4.1. 5-(4-(methyl(prop-2-yn-1-yl)amino)butoxy)-2,3-dihydro-1H-inden-1-one (**6a**)*

Yield 83%; pale yellow oil; ^1H NMR (500 MHz, $CDCl_3$) δ 7.68–7.63 (m, 1H), 6.87 (d, J = 5.4 Hz, 2H), 4.04 (t, J = 6.3 Hz, 2H), 3.36 (d, J = 2.2 Hz, 2H), 3.12–3.02 (m, 2H), 2.69–2.61 (m, 2H), 2.54–2.47 (m, 2H), 2.32 (s, 3H), 2.22 (t, J = 2.2 Hz, 1H), 1.89–1.80 (m, 2H), 1.72–1.61 (m, 2H). ^{13}C NMR (126 MHz, $CDCl_3$) δ 205.45 (s), 164.83 (s), 158.27 (s), 130.35 (s), 125.42 (s), 115.74 (s), 110.36 (s), 78.38 (s), 73.41 (s), 68.17 (s), 55.18 (s), 45.59 (s), 41.75 (s), 36.53 (s), 26.95 (s), 25.97 (s), 24.03 (s). HRMS: calcd for $C_{17}H_{21}NO_2$ $[M+H]^+$ 272.1645, found 272.1658.

*4.4.2. 5-((5-(methyl(prop-2-yn-1-yl)amino)pentyl)oxy)-2,3-dihydro-1H-inden-1-one (**6b**)*

Yield 87%; pale yellow oil; ^1H NMR (500 MHz, $CDCl_3$) δ 7.68–7.62 (m, 1H), 6.89–6.83 (m, 2H), 4.01 (t, J = 6.4 Hz, 2H), 3.34 (d, J = 2.3 Hz, 2H), 3.09 – 3.02 (m, 2H), 2.68–2.60 (m, 2H), 2.47–2.43 (m, 2H), 2.31 (s, 3H), 2.22 (t, J = 2.3 Hz, 1H), 1.88–1.77 (m, 2H), 1.59–1.45 (m, 4H). ^{13}C NMR (126 MHz, $CDCl_3$) δ 205.45 (s), 164.87 (s), 158.28 (s), 130.30 (s), 125.41 (s), 115.73 (s), 110.31 (s), 78.40 (s), 73.38 (s), 68.33 (s), 55.53 (s), 45.58 (s), 41.82 (s), 36.52 (s), 29.04 (s), 27.29 (s), 25.96 (s), 23.92 (s). HRMS: calcd for $C_{18}H_{23}NO_2$ $[M+H]^+$ 286.1802, found 286.1813.

*4.4.3. 5-((6-(methyl(prop-2-yn-1-yl)amino)hexyl)oxy)-2,3-dihydro-1H-inden-1-one (**6c**)*

Yield 78%; pale yellow solid; m.p. 52.7-53.2 ^oC; ^1H NMR (500 MHz, $CDCl_3$) δ 7.68–

7.64 (m, 1H), 6.87 (d, *J* = 4.9 Hz, 2H), 4.01 (t, *J* = 6.5 Hz, 2H), 3.34 (d, *J* = 2.2 Hz, 2H), 3.10–3.03 (m, 2H), 2.69–2.60 (m, 2H), 2.48–2.38 (m, 2H), 2.30 (s, 3H), 2.21 (t, *J* = 2.2 Hz, 1H), 1.87–1.76 (m, 2H), 1.49 (dq, *J* = 14.5, 7.2 Hz, 4H), 1.39 (dd, *J* = 14.3, 7.5 Hz, 2H). ^{13}C NMR (126 MHz, $CDCl_3$) δ 205.43 (s), 164.92 (s), 158.27 (s), 130.30 (s), 125.41 (s), 115.74 (s), 110.34 (s), 78.48 (s), 73.31 (s), 68.41 (s), 55.64 (s), 45.57 (s), 41.84 (s), 36.52 (s), 29.12 (s), 27.53 (s), 27.19 (s), 26.02 (s), 25.96 (s). HRMS: calcd for $C_{19}H_{25}NO_2$ $[M+H]^+$ 300.1958, found 300.1961.

*4.4.4. 6-((6-(methyl(prop-2-yn-1-yl)amino)hexyl)oxy)benzofuran-3(2H)-one (**6d**)*

Yield 86%; yellow oil; ^{1}H NMR (500 MHz, $CDCl_3$) δ 7.55 (d, *J* = 8.6 Hz, 1H), 6.63 (dd, *J* = 8.6, 1.7 Hz, 1H), 6.51 (d, *J* = 1.5 Hz, 1H), 4.61 (s, 2H), 4.01 (t, *J* = 6.4 Hz, 2H), 3.41 (s, 2H), 2.55 – 2.47 (m, 2H), 2.37 (s, 3H), 2.27 (s, 1H), 1.86 – 1.77 (m, 2H), 1.55 (dd, *J* = 15.0, 7.5 Hz, 2H), 1.51 – 1.46 (m, 2H), 1.43 – 1.36 (m, 2H). ^{13}C NMR (126 MHz, $CDCl_3$) δ 196.72 (s), 175.69 (s), 166.88 (s), 124.18 (s), 113.28 (s), 111.20 (s), 95.88 (s), 74.67 (s), 73.06 (s), 67.77 (s), 54.53 (s), 44.44 (s), 40.66 (s), 27.96 (s), 26.20 (s), 26.12 (s), 24.97 (s). HRMS: calcd for $C_{18}H_{23}NO_3$ $[M+H]^+$ 302.1751, found 302.1764.

*4.4.5. 6-(4-(methyl(prop-2-yn-1-yl)amino)butoxy)-3,4-dihydronaphthalen-1(2H)-one (**6e**)*

Yield 91%; pale yellow oil; ^{1}H NMR (500 MHz, $CDCl_3$) δ 7.96 (d, *J* = 8.7 Hz, 1H), 6.78 (dd, *J* = 8.7, 1.9 Hz, 1H), 6.67 (s, 1H), 4.01 (t, *J* = 6.3 Hz, 2H), 3.34 (d, *J* = 1.8 Hz, 2H), 2.88 (t, *J* = 6.0 Hz, 2H), 2.60 – 2.54 (m, 2H), 2.47 (t, *J* = 7.3 Hz, 2H), 2.30 (s, 3H), 2.21 (s, 1H), 2.12 – 2.04 (m, 2H), 1.86 – 1.77 (m, 2H), 1.68 – 1.57 (m, 2H). ^{13}C NMR (126 MHz, $CDCl_3$) δ 197.30 (s), 163.10 (s), 147.00 (s), 129.66 (s), 126.22 (s), 113.50 (s), 113.18 (s), 78.46 (s), 77.16 (s), 73.30 (s), 67.87 (s), 55.16 (s), 45.57 (s), 41.73 (s), 38.96 (s), 30.22 (s), 26.95 (s), 24.02 (s), 23.45 (s). HRMS: calcd for $C_{18}H_{23}NO_2$ $[M+H]^+$ 286.1801, found 286.1815.

4.4.6.

*6-((5-(methyl(prop-2-yn-1-yl)amino)pentyl)oxy)-3,4-dihydronaphthalen-1(2H)-one (**6f**)*

Yield 76%; pale yellow oil; ^{1}H NMR (500 MHz, $CDCl_3$) δ 7.96 (d, *J* = 8.7 Hz, 1H),

6.77 (dd, *J* = 8.7, 2.1 Hz, 1H), 6.66 (d, *J* = 1.4 Hz, 1H), 3.98 (t, *J* = 6.4 Hz, 2H), 3.32 (d, *J* = 2.1 Hz, 2H), 2.88 (t, *J* = 6.0 Hz, 2H), 2.59 – 2.54 (m, 2H), 2.42 (t, *J* = 7.1 Hz, 2H), 2.29 (s, 3H), 2.21 (t, *J* = 2.0 Hz, 1H), 2.11 – 2.03 (m, 2H), 1.85 – 1.75 (m, 2H), 1.56 – 1.42 (m, 4H). ^{13}C NMR (126 MHz, $CDCl_3$) δ 197.31 (s), 163.14 (s), 147.00 (s), 129.65 (s), 126.18 (s), 113.48 (s), 113.14 (s), 78.47 (s), 73.27 (s), 68.02 (s), 55.50 (s), 45.55 (s), 41.79 (s), 38.94 (s), 30.20 (s), 29.03 (s), 27.28 (s), 23.88 (s), 23.43 (s). HRMS: calcd for $C_{19}H_{25}NO_2$ $[M+H]^+$ 300.1958, found 300.1970.

4.4.7.

6-((6-(methyl(prop-2-yn-1-yl)amino)hexyl)oxy)-3,4-dihydronaphthalen-1(2H)-one ***(6g)***

Yield 74%; pale yellow oil; ^{1}H NMR (500 MHz, $CDCl_3$) δ 7.97 (d, *J* = 8.7 Hz, 1H), 6.78 (dd, *J* = 8.7, 2.4 Hz, 1H), 6.67 (d, *J* = 2.2 Hz, 1H), 3.98 (t, *J* = 6.5 Hz, 2H), 3.34 (d, *J* = 2.3 Hz, 2H), 2.89 (t, *J* = 6.1 Hz, 2H), 2.58 (t, *J* = 6.5 Hz, 2H), 2.42 (t, *J* = 6.5 Hz, 2H), 2.30 (s, 3H), 2.21 (t, *J* = 2.3 Hz, 1H), 2.14–2.04 (m, 2H), 1.84–1.74 (m, 2H), 1.48 (m, 4H), 1.38 (m, 2H). ^{13}C NMR (126 MHz, $CDCl_3$) δ 197.35 (s), 163.21 (s), 147.02 (s), 129.68 (s), 126.19 (s), 113.50 (s), 113.19 (s), 78.45 (s), 73.31 (s), 68.11 (s), 55.63 (s), 45.54 (s), 41.81 (s), 38.98 (s), 30.24 (s), 29.13 (s), 27.50 (s), 27.18 (s), 26.00 (s), 23.47 (s). HRMS: calcd for $C_{20}H_{27}NO_2$ $[M+H]^+$ 314.2114, found 314.2127.

4.4.8. 7-(3-(methyl(prop-2-yn-1-yl)amino)propoxy)chroman-4-one ***(6h)***

Yield 81%; yellow solid; m.p. 55.1-56.7 ^{o}C; ^{1}H NMR (500 MHz, $CDCl_3$) δ 7.81 (d, *J* = 8.8 Hz, 1H), 6.56 (dd, *J* = 8.8, 2.2 Hz, 1H), 6.39 (d, *J* = 2.2 Hz, 1H), 4.49 (t, *J* = 6.4 Hz, 2H), 4.03 (t, *J* = 6.3 Hz, 2H), 3.36 (d, *J* = 2.2 Hz, 2H), 2.73 (t, *J* = 6.4 Hz, 2H), 2.60 (t, *J* = 7.1 Hz, 2H), 2.33 (s, 3H), 2.23 (t, *J* = 2.3 Hz, 1H), 1.95 (p, *J* = 6.6 Hz, 2H). ^{13}C NMR (126 MHz, $CDCl_3$) δ 190.65 (s), 165.49 (s), 163.87 (s), 128.93 (s), 115.29 (s), 110.33 (s), 101.37 (s), 78.27 (s), 73.52 (s), 67.46 (s), 66.47 (s), 52.13 (s), 45.75 (s), 41.76 (s), 37.53 (s), 27.14 (s). HRMS: calcd for $C_{16}H_{19}NO_3$ $[M+H]^+$ 274.1438, found 274.1438.

4.4.9. 7-(4-(methyl(prop-2-yn-1-yl)amino)butoxy)chroman-4-one ***(6i)***

Yield 71%; pale yellow oil; ^{1}H NMR (500 MHz, $CDCl_3$) δ 7.82 (d, *J* = 8.8 Hz, 1H), 6.56 (dd, *J* = 8.8, 2.4 Hz, 1H), 6.38 (d, *J* = 2.3 Hz, 1H), 4.50 (t, *J* = 6.3 Hz, 2H), 4.00

(t, *J* = 6.3 Hz, 2H), 3.37 (d, *J* = 2.3 Hz, 2H), 2.74 (t, *J* = 5.0 Hz, 2H), 2.50 (t, *J* = 5.0 Hz, 2H), 2.33 (s, 3H), 2.23 (t, *J* = 2.4 Hz, 1H), 1.87–1.77 (m, 2H), 1.64 (m, 2H). ^{13}C NMR (126 MHz, $CDCl_3$) δ 190.77 (s), 165.63 (s), 163.78 (s), 128.95 (s), 115.29 (s), 110.31 (s), 101.28 (s), 78.01 (s) 73.69 (s), 68.09 (s), 67.43 (s), 55.06 (s), 45.73 (s), 42.00 (s), 37.29 (s), 27.07 (s), 23.98 (s). HRMS: calcd for $C_{17}H_{21}NO_3$ $[M+H]^+$ 288.1594, found 288.1568.

*4.4.10. 7-((5-(methyl(prop-2-yn-1-yl)amino)pentyl)oxy)chroman-4-one (**6j**)*

Yield 89%; yellow oil; ^{1}H NMR (500 MHz, $CDCl_3$) δ 7.82 (d, *J* = 8.8 Hz, 1H), 6.55 (dd, *J* = 8.8, 2.4 Hz, 1H), 6.38 (d, *J* = 2.3 Hz, 1H), 4.50 (t, *J* = 6.4 Hz, 2H), 3.98 (t, *J* = 6.4 Hz, 2H), 3.37 (d, *J* = 2.3 Hz, 2H), 2.74 (t, *J* = 5.0 Hz 2H), 2.47 (t, *J* = 5.0 Hz, 2H), 2.33 (s, 3H), 2.24 (t, *J* = 2.4 Hz, 1H), 1.81 (q, *J* = 6.6 Hz, 2H), 1.60–1.52 (m, 2H), 1.48 (m, 2H). ^{13}C NMR (126 MHz, $CDCl_3$) δ 190.76 (s), 165.61 (s), 163.90 (s), 128.97 (s), 115.30 (s), 110.32 (s), 101.29 (s), 78.27 (s), 73.69 (s), 68.35 (s), 67.49 (s), 55.53 (s), 45.59 (s), 41.82 (s), 37.57 (s), 28.98 (s), 27.38 (s), 23.92 (s). HRMS: calcd for $C_{18}H_{23}NO_3$ $[M+H]^+$ 302.1751, found 302.1745.

*4.4.11. 7-((6-(methyl(prop-2-yn-1-yl)amino)hexyl)oxy)chroman-4-one (**6k**)*

Yield 73%; pale yellow oil; ^{1}H NMR (500 MHz, $CDCl_3$) δ 7.82 (d, *J* = 8.8 Hz, 1H), 6.56 (dd, *J* = 8.8, 2.3 Hz, 1H), 6.38 (d, *J* = 2.3 Hz, 1H), 4.58–4.45 (m, 2H), 3.97 (t, *J* = 6.4 Hz, 2H), 3.46 (s, 2H), 2.79–2.70 (m, 2H), 2.62–2.51 (m, 2H), 2.42 (s, 3H), 2.31 (s, 1H), 1.86–1.73 (m, 2H), 1.58 (dt, *J* = 15.0, 7.6 Hz, 2H), 1.52–1.45 (m, 2H), 1.40 (dd, *J* = 15.1, 8.1 Hz, 2H). ^{13}C NMR (126 MHz, $CDCl_3$) δ 190.69 (s), 165.63 (s), 163.92 (s), 128.98 (s), 115.26 (s), 110.39 (s), 101.31 (s), 68.37 (s), 67.50 (s), 55.47 (s), 45.34 (s), 41.52 (s), 37.57 (s), 29.01 (s), 27.07 (s), 25.94 (s), 26.93. HRMS: calcd for $C_{19}H_{25}NO_3$ $[M+H]^+$ 316.1907, found 316.1913.

*4.4.12. 7-((8-(methyl(prop-2-yn-1-yl)amino)octyl)oxy)chroman-4-one (**6l**)*

Yield 89%; pale yellow oil; ^{1}H NMR (500 MHz, $CDCl_3$) δ 7.82 (d, *J* = 8.8 Hz, 1H), 6.56 (dd, *J* = 8.8, 2.3 Hz, 1H), 6.38 (d, *J* = 2.3 Hz, 1H), 4.50 (t, *J* = 6.4 Hz, 2H), 3.97 (t, *J* = 6.5 Hz, 2H), 3.39 (d, *J* = 2.1 Hz, 2H), 2.74 (t, *J* = 5.0 Hz, 2H), 2.46 (t, *J* = 5.0 Hz, 2H), 2.35 (s, 3H), 2.25 (t, *J* = 2.3 Hz, 1H), 1.77 (m, 2H), 1.55–1.40 (m, 4H), 1.33 (br, 6H). ^{13}C NMR (126 MHz, $CDCl_3$) δ 190.68 (s), 165.69 (s), 163.91 (s), 128.95 (s),

115.21 (s), 110.41 (s), 101.29 (s), 77.90 (s), 73.84 (s), 68.52 (s), 67.48 (s), 55.73 (s), 45.47 (s), 41.71 (s), 37.57 (s), 29.50 (s), 29.34 (s), 29.07 (s), 27.37 (s), 26.01 (s). HRMS: calcd for $C_{21}H_{29}NO_3$ $[M+H]^+$ 344.2220, found 344.2221.

*4.4.13. 1-(4-(4-(methyl(prop-2-yn-1-yl)amino)butoxy)phenyl)ethan-1-one (**6m**)*

Yield 81%; pale yellow oil; ^{1}H NMR (500 MHz, DMSO-d6) δ 7.91 (d, J = 8.8 Hz, 2H), 7.02 (d, J = 8.8 Hz, 2H), 4.06 (t, J = 6.5 Hz, 2H), 3.29 (s, 3H), 3.10 (s, 1H), 2.39 (t, J = 7.1 Hz, 2H), 2.19 (s, 3H), 1.78–1.68 (m, 2H), 1.53 (dt, J = 14.6, 7.3 Hz, 2H), 1.34 (s, 2H). ^{13}C NMR (126 MHz, DMSO) δ 196.32 (s), 162.55 (s), 130.51 (s), 129.75 (s), 114.28 (s), 75.77 (s), 67.70 (s), 54.45 (s), 44.89 (s), 41.18 (s), 29.80 (s), 26.42 (s), 26.31 (s), 23.24 (s). HRMS: calcd for $C_{16}H_{21}NO_2$ $[M+H]^+$ 260.1645, found 260.1651.

*4.4.14. 1-(4-((6-(methyl(prop-2-yn-1-yl)amino)hexyl)oxy)phenyl)ethan-1-one (**6n**)*

Yield 74%; pale yellow oil;^{1}H NMR (500 MHz, DMSO-d6) δ 8.00–7.80 (m, 2H), 7.09–6.93 (m, 2H), 4.04 (t, J = 6.5 Hz, 2H), 3.27 (s, 3H), 3.09 (s, 1H), 2.32 (t, J = 7.1 Hz, 2H), 2.17 (s, 3H), 1.77–1.68 (m, 2H), 1.43–1.36 (m, 4H), 1.35–1.27 (m, 4H). ^{13}C NMR (126 MHz, DMSO) δ 196.31 (s), 162.58 (s), 130.50 (s), 129.74 (s), 114.26 (s), 75.68 (s), 67.85 (s), 54.87 (s), 44.90 (s), 41.29 (s), 28.53 (s), 26.79 (s), 26.55 (s), 26.42 (s), 25.36 (s). HRMS: calcd for $C_{18}H_{25}NO_2$ $[M+H]^+$ 288.1958, found 288.1966.

*4.4.15. 5-(3-methoxyphenoxy)-N-methyl-N-(prop-2-yn-1-yl)pentan-1-amine (**6o**)*

Yield 84%; pale yellow oil; ^{1}H NMR (500 MHz, DMSO-d6) δ 7.15 (t, J = 8.2 Hz, 1H), 6.50 (t, J = 2.5 Hz, 1H), 6.48 (t, J = 2.4 Hz, 1H), 6.46 (t, J = 2.3 Hz, 1H), 3.92 (t, J = 6.5 Hz, 2H), 3.72 (s, 3H), 3.10 (s, 1H), 2.35 (s, 2H), 2.18 (s, 3H), 1.69 (dd, J = 12.8, 5.9 Hz, 2H), 1.46–1.38 (m, 4H), 1.35 (d, J = 2.6 Hz, 2H). ^{13}C NMR (126 MHz, DMSO) δ 160.94 (s), 160.39 (s), 130.37 (s), 107.03 (s), 106.61 (s), 101.07 (s), 67.81 (s), 55.51 (s), 55.28 (s), 45.33 (s), 30.24 (s), 29.00 (s), 23.83 (s). HRMS: calcd for $C_{16}H_{23}NO_2$ $[M+H]^+$ 262.1801, found 266.1809.

*4.4.16. 1-(3-methoxy-4-(4-(methyl(prop-2-yn-1-yl)amino)butoxy)phenyl)ethan-1-one (**6p**)*

Yield 75%; pale yellow solid; m.p. 65.1-65.9 ^{o}C; ^{1}H NMR (500 MHz, $CDCl_3$) δ 7.54 (dd, J = 8.3, 2.0 Hz, 1H), 7.50 (d, J = 2.0 Hz, 1H), 6.87 (d, J = 8.4 Hz, 1H), 4.10 (t, J

= 6.6 Hz, 2H), 3.90 (s, 3H), 3.35 (d, *J* = 2.4 Hz, 2H), 2.55 (s, 3H), 2.51 – 2.45 (m, 2H), 2.31 (s, 3H), 2.21 (t, *J* = 2.4 Hz, 1H), 1.89 (dd, *J* = 14.9, 6.8 Hz, 2H), 1.65 (dt, *J* = 15.0, 7.5 Hz, 2H). ^{13}C NMR (126 MHz, $CDCl_3$) *δ* 196.71 (s), 152.70 (s), 149.08 (s), 130.14 (s), 123.09 (s), 111.01 (s), 110.25 (s), 78.27 (s), 72.91 (s), 68.39 (s), 55.86 (s), 54.81 (s), 45.35 (s), 41.50 (s), 26.60 (s), 25.99 (s), 23.59 (s). HRMS: calcd for $C_{17}H_{23}NO_3$ $[M+H]^+$ 290.1751, found 290.1749.

4.4.17.

*1-(3-methoxy-4-((5-(methyl(prop-2-yn-1-yl)amino)pentyl)oxy)phenyl)ethan-1-one (**6q**)*

Yield 79%; yellow oil; ^{1}H NMR (500 MHz, $CDCl_3$) *δ* 7.54 (dd, *J* = 8.3, 2.0 Hz, 1H), 7.50 (d, *J* = 2.0 Hz, 1H), 6.87 (d, *J* = 8.4 Hz, 1H), 4.10 (t, *J* = 6.6 Hz, 2H), 3.90 (s, 3H), 3.35 (d, *J* = 2.4 Hz, 2H), 2.55 (s, 3H), 2.51–2.45 (m, 2H), 2.31 (s, 3H), 2.21 (t, *J* = 2.4 Hz, 1H), 1.89 (dd, *J* = 14.9, 6.8 Hz, 2H), 1.65 (dt, *J* = 15.0, 7.5 Hz, 2H). ^{13}C NMR (126 MHz, $CDCl_3$) *δ* 196.98 (s), 152.98 (s), 149.29 (s), 130.28 (s), 123.49 (s), 111.09 (s), 110.55 (s), 78.51 (s), 73.31 (s), 68.97 (s), 56.13 (s), 55.54 (s), 45.61 (s), 41.84 (s), 28.96 (s), 27.30 (s), 26.34 (s), 23.88 (s). HRMS: calcd for $C_{18}H_{25}NO_3$ $[M+H]^+$ 304.1907, found 304.1908.

*4.4.18. 2-methoxy-4-(4-(methyl(prop-2-yn-1-yl)amino)butoxy)benzaldehyde (**6r**)*

Yield 79%; red solid; m.p. 83.6-84.2 ^{o}C; ^{1}H NMR (500 MHz, $CDCl_3$) *δ* 10.26 (s, 1H), 7.78 (d, *J* = 8.7 Hz, 1H), 6.52 (dd, *J* = 8.7, 1.9 Hz, 1H), 6.43 (d, *J* = 2.0 Hz, 1H), 4.04 (t, *J* = 6.3 Hz, 2H), 3.88 (s, 3H), 3.36 (s, 2H), 2.53–2.47 (m, 2H), 2.32 (s, 3H), 2.22 (t, *J* = 2.3 Hz, 1H), 1.88–1.79 (m, 2H), 1.70–1.60 (m, 2H). ^{13}C NMR (126 MHz, $CDCl_3$) *δ* 188.48 (s), 165.80 (s), 163.71 (s), 130.85 (s), 119.01 (s), 106.28 (s), 98.45 (s), 78.38 (s), 73.42 (s), 68.17 (s), 55.71 (s), 55.16 (s), 45.60 (s), 41.77 (s), 26.96 (s), 24.02 (s). HRMS: calcd for $C_{16}H_{21}NO_3$ $[M+H]^+$ 276.1594, found 276.1601.

*4.4.19. 2-methoxy-4-((5-(methyl(prop-2-yn-1-yl)amino)pentyl)oxy)benzaldehyde (**6s**)*

Yield 82%; yellow solid; m.p. 51.2-51.6 ^{o}C; ^{1}H NMR (500 MHz, $CDCl_3$) *δ* 10.24 (s, 1H), 7.76 (d, *J* = 8.7 Hz, 1H), 6.49 (dd, *J* = 8.7, 1.8 Hz, 1H), 6.41 (d, *J* = 1.9 Hz, 1H), 4.00 (t, *J* = 6.4 Hz, 2H), 3.87 (s, 3H), 3.33 (d, *J* = 2.2 Hz, 2H), 2.43 (t, *J* = 7.1 Hz, 2H), 2.37 (s, 1H), 2.29 (s, 3H), 2.21 (t, *J* = 2.2 Hz, 1H), 1.87–1.76 (m, 2H), 1.50 (t, *J* = 11.4 Hz, 4H). ^{13}C NMR (126 MHz, $CDCl_3$) *δ* 188.44 (s), 165.82 (s), 163.68 (s),

130.79 (s), 118.92 (s), 106.24 (s), 98.38 (s), 78.48 (s), 73.29 (s), 68.33 (s), 55.66 (s), 55.50 (s), 45.56 (s), 41.81 (s), 29.02 (s), 27.29 (s), 23.89 (s). HRMS: calcd for $C_{17}H_{23}NO_3$ $[M+H]^+$ 290.1751, found 290.1764.

*4.4.20. 2-methoxy-4-((6-(methyl(prop-2-yn-1-yl)amino)hexyl)oxy)benzaldehyde (**6t**)*

Yield 73%; yellow power; m.p. 57.5-57.9 ^oC;^1H NMR (500 MHz, $CDCl_3$) δ 10.26 (s, 1H), 7.77 (d, J = 8.7 Hz, 1H), 6.51 (dd, J = 8.7, 1.5 Hz, 1H), 6.42 (d, J = 1.8 Hz, 1H), 4.00 (t, J = 6.5 Hz, 2H), 3.88 (s, 3H), 3.34 (d, J = 2.1 Hz, 2H), 2.48–2.38 (m, 2H), 2.30 (s, 3H), 2.21 (t, J = 2.2 Hz, 1H), 1.85–1.74 (m, 2H), 1.55–1.44 (m, 4H), 1.39 (dd, J = 14.5, 7.6 Hz, 2H). ^{13}C NMR (126 MHz, $CDCl_3$) δ 188.44 (s), 165.87 (s), 163.70 (s), 130.82 (s), 118.94 (s), 106.26 (s), 98.41 (s), 78.47 (s), 73.31 (s), 68.41 (s), 55.64 (s), 45.57 (s), 41.83 (s), 29.14 (s), 27.53 (s), 27.19 (s), 26.01 (s). HRMS: calcd for $C_{18}H_{25}NO_3$ $[M+H]^+$ 304.1907, found 304.1921.

4.5. MAO inhibition assay

The potential effects of all the synthesized compounds **6a**-**6t** on MAOs activity was investigated according to preciously reported fluorescence methods [57-58]. The experiment was measuring the production of H_2O_2 from *p*-tyramine, using recombinant human MAOs and Amplex Red assay kit. The enzyme of *h*MAO-A and *h*MAO-B was obtained from Sigma-Aldrich (St. Louis, MO, USA), and *p*-tyramine was purchased from Molecular Probes, Inc. (Eugene, Oregon, USA). Each synthetic compound was adjusted with DMSO and PBS buffer solution to different final concentrations (DMSO < 0.1%). The test compound was combined with *h*MAO-A (or hMAO-B) and other substrate, and then incubated for 15 min at 37 ^oC in a 96-well black microtiter plate in the dark. The results were tested by a multidetection microplate fluorescence reader at excitation/emission wavelengths of 545/590 nm. Data were shown as mean ± SD of three independent experiments.

4.6 Molecular modeling studies

Molecular modeling studies were carried out using the Chemical Computing Group's Molecular Operating Environment (MOE) software (Montreal, Canada, version 2015.10). The docking template structure of MAO-B was derived from the X-ray crystal structure of the human MAO-B in complex with

7-(3-chlorobenzyloxy)-4-(methylamino)methyl-coumarin (PDB code 2V61) and all water molecules were removed. The protein was energy minimized and 3D protonated using the structure preparation module of MOE. Ligand file for the molecular docking studies was prepared in MOE and energy minimized using Merck Molecular force field (MMFF94x, RMSD gradient: 0.05 kcal mol^{-1} $Å^{-1}$). Then, the optimized geometry of ligand was saved in a molecular database file and docked into the active site of the protein using the MOE-Dock program. The London dG was chosen as initial scoring method and Rigid Receptor was selected as the final scoring method. Finally, the geometry of docked complex was analyzed by the pose viewer utility in MOE.

4.7. Reversibility and kinetic study of hMAO-B inhibition

The reversibility experiment of compound **6j** for MAO-B was performed according to a previously reported method [59]. Compound **6j** at concentrations of $10\times IC_{50}$ and $100\times IC_{50}$ was treated with *h*MAO-B enzyme (0.75 mg/mL) for 30 min at 37 ^{o}C. The parallel control was without compound **6j** under the same condition. Then, the concentrations of compound **6j** was diluted to 100-fold respectively. Pargyline at concentration of $10\times IC_{50}$ was diluted to $0.1 \times IC_{50}$ by the same times.

Lineweaver-Burk reciprocal plots revealed *h*MAO-B inhibition mechanism of compound **6j**. Compound **6j** at three different concentrations (2.5, 5 and 10 nM) were for kinetic study. The initial catalytic rates of *h*MAO-B were tested in the presence or absence of compound **6j** at the corresponding concentrations with different concentrations (0.05, 0.1, 0.5, 1.0, 1.5, and 3.0 mM) of *p*-tyramine. The results were analyzed by Graph Pad Prism 4.03 software (San Diego, CA, USA).

4.8. Inhibition of self-induced $A\beta_{1-42}$ aggregation

A thioflavin T (ThT)-binding assay [60] was used to measure the inhibition of self-induced $A\beta_{1-42}$ aggregation. Curcumin was the reference compounds. $A\beta_{1-42}$ was aliquoted and stored at -80 ^{o}C. Before the experiment of compounds inhibiting self-induced $A\beta_{1-42}$ aggregation, $A\beta_{1-42}$ stock solution was diluted to 50 mM with 50 mM phosphate buffer (ph = 7.4). $A\beta_{1-42}$ solution (10 mL, 25 mM, final concentration) in the presence or absence of compound (10 mL) was incubated at 37 ^{o}C for 48 h.

Using 50 mM phosphate buffer (pH 7.4) instead of $A\beta_{1-42}$ in the presence or absence of inhibitors as blanks. The sample was diluted to final volume of 200 mL using 50 mM glycine-NaOH buffer (pH 8.0) containing thioflavin T (5 mM). Then we detected the fluorescence intensities 5 min later (excitation, 446 nm; emission, 490 nm). The calculation formula was (1-IFi/IFc)*100%. IFi and IFc were the fluorescence intensities, which was $A\beta_{1-42}$ in the presence and absence of inhibitors after subtracting the background, respectively.

4.9. In vitro blood brain barrier permeation assay

Parallel artificial membrane permeation assay (PAMPA) was used to tested the blood brain barrier(BBB) permeability of all synthesized compounds. The materials of experiment included commercial drugs (from Sigma and Alfa Aesar), porcine brain lipid (PBL, Avanti Polar Lipids), donor microplate (PVDF membrane, pore size 0.45 mm), the acceptor microplate and the 96-well UV plate (Corning Incorporated). Filter membrane was coated with PBL(4 ml) in dodecane (20 mg/mL) and acceptor 96-well microplate with 300 mL of PBS/EtOH (7:3). Compounds diluted to 100 mg/mL concentration using DMSO (<0.1%) and PBS/EtOH (7:3) solution, and then added to donor wells. The donor ate and acceptor filter was formed a sandwich and was undisturbed for 16 h at 25 ^{o}C. The concentration of compound in the acceptor wells was tested by a UV plate reader (Flexstation@ 3). Commercial drugs with BBB permeability were also detected as controls.

4.10. SH-SY5Y neuroblastoma cell toxicity assay

The cytotoxicity effect of compound **6j** on SH-SY5Y neuroblastoma cells were tested by MTT according to previously reported method [61]. The human neuroblastoma SH-SY5Y cells were cultured in DMEM supplemented with fetal bovine serum (FBS), 100 U/mL penicillin and 100 μg/mL streptomycin with 5% CO_2 in air at 37 ^{o}C. A density of 10,000 SH-SY5Y cell were seeded into 96-well plates, and then different concentrations of compound **6j** (6.25–100 μM) or rasagiline were also added into 96-well plates. After they were incubated at 37 °C for 24 hours, 20 μL MTT was added into 96-well plates, and the mixture was incubated at 37 °C for 4 h. Subsequently, we removed the medium and added 200 μL DMSO to dissolve the

MTT formazan crystal. We used a microculture plate reader to test each well absorbance at a wavelength of 570 nm and a reference wavelength of 630 nm. All experiment data was presented as the mean±SD of three independent experiments.

4.11. Pharmacokinetics assay in Sprague-Dawley rats [62]

The pharmacokinetic parameter of male SD rats' compound **6j** was measured by intravenous injection and oral administration was studied. Male SD rats (n=3, 220 ± 20 g) received compound **6j** by intravenous injection (3 mg/kg) or orally gavage (10 mg/kg). We collected a serial of samples at appropriate intervals (0.083, 0.17, 0.5, 1, 1.5, 2, 4, 6, 8, 12, 24, 36 and 48 h post dose). Samples were centrifuged at 10000 rpm for 2 min and stored at -20 ^{o}C. Plasma proteins were precipitated using two volumes of 0.5% formic acid/acetonitrile (v/v). The supernatants after centrifugation (14000 rpm, 14 min) were analyzed by LC-MS/MS (Waters, ACQUITY-TQ-XS). PK parameters were calculated via DAS 2.0 software (China).

Acknowledgement

This work was supported by National Natural Science Foundation of China [No. 31970371, 81760622, 21807052, 31600265, 81973533]; Guangxi Science and Technology Base and Special Talents Program [Grant No. AD18281032]; Support Program for Outstanding Youth Talents in Jiangxi province [Grant No. 20192BCB23018]; the Program of Natural Science Foundation of Jiangxi Province of China [Grant No. 20192ACBL21034]; 1050 Young talents project of Jiangxi University of Traditional Chinese Medicine [Grant No. 1141900616]; The program of first-class disciplines in Chinese Medicine of Jiangxi Province [Grant No. JXSYLXK-ZHYAO047]; the Natural Science Foundation of Guangxi Zhuang Autonomous Region of China [No. 2017GXNSFAA198077].

References

[1] P. Marešová, H. Mohelská, J. Dolejš, K. Kuča, Socio-economic Aspects of Alzheimer's Disease, Current Alzheimer Research, 2015, 12, 903-911.

[2] R. Cimler, P. Maresova, J. Kuhnova, K. Kuca, Predictions of Alzheimer’s disease

treatment and care costs in European countries, PloS ONE, 2019, 14(1), 210958-210973.

[3] R.M. Anderson, C. Hadjichrysanthou, S. Evans, M.M. Wong, Why do so many clinical trials of therapies for Alzheimer's disease fail? Lancet 390 (2017) 2327–2329.

[4] R. Cacabelos, Have there been improvements in Alzheimer's disease drug discovery over the past 5 years? Expert Opin. Drug Discov. 13 (2018) 523–538.

[5] A. Wimo, L. Jonsson, J. Bond, M. Prince, B. Winblad, The worldwide economic impact of dementia 2010, Alzheimer’s & Dementia 9 (2013) 1–11.

[6] H.W. Querfurth, F.M. LaFerla, Alzheimer’s Disease, N. Engl. J. Med. 362 (2010) 329−344.

[7] S. Carradori, R. Silvestri, New frontiers in selective human MAO-B inhibitors, J. Med. Chem. 58 (2015) 6717–6732.

[8] S. Chakrabarti, M. Sinha, I.G. Thakurta, P. Banerjee, M. Chattopadhyay, Oxidative Stress and Amyloid Beta Toxicity in Alzheimer’s Disease: Intervention in a Complex Relationship by Antioxidants. Curr. Med. Chem. 20 (2013) 4648−4664.

[9] N. Jiang, S.Y. Li, S.S. Xie, Z.R. Li, K.D.G. Wang, X.B. Wang, L.Y. Kong, Design, synthesis and evaluation of multifunctional salphen derivatives for the treatment of Alzheimer's disease, Eur. J. Med. Chem. 87 (2014) 540-551.

[10] N. Jiang, X.B. Wang, Z.R. Li, S.S. Xie, M. Huang, L.Y. Kong, Design of a structural framework with potential use to develop balanced multifunctional agents against Alzheimer's disease, Rsc. Adv. 5 (2015) 14242-14255.

[11] N. Desideri, L.P. Monaco, R. Fioravanti, M. Biava, M. Yáñez, S. Alcaro, F. Ortuso, (E)-3-Heteroarylidenechroman-4-ones as potent and selective monoamine oxidase-B inhibitors, Eur. J. Med. Chem. 117 (2016) 292-300.

[12] L. Pisani, R. Farina, M. Catto, R.M. Iacobazzi, O. Nicolotti, S. Cellamare, G.F. Mangiatordi, N. Denora, R. Soto-Otero, L. Siragusa, C.D. Altomare, A. Carotti, Exploring Basic Tail Modifications of Coumarin-based Dual Acetylcholinesterase-Monoamine Oxidase B Inhibitors: Identification of Water-soluble, Brain-permeant Neuroprotective Multitarget Agents, J. Med. Chem. 59 (2016) 6791-6806.

[13] H.L. Yang, P. Cai, Q.H. Liu, X.L. Yang, F. Li, J. Wang, J.J. Wu, X.B. Wang, L.Y. Kong. Design, synthesis and evaluation of coumarin-pargyline hybrids as novel dual inhibitors of monoamine oxidases and amyloid-β aggregation for the treatment of Alzheimer's disease, Eur. J. Med. Chem. 138 (2017) 715-728.

[14] M.G. Savelieff, G. Nam, J. Kang, H.J. Lee, M. Lee, M.H. Lim, Development of Multifunctional Molecules as Potential Therapeutic Candidates for Alzheimer's Disease, Parkinson' s Disease, and Amyotrophic Lateral Sclerosis in the Last Decade, Chem. Rev. 119 (2019) 1221−1322.

[15] R. Farina, L. Pisani, M. Catto, O. Nicolotti, D. Gadaleta, N. Denora, R. Soto-Otero, E. Méndez-Álvarez, C.S. Passos, G. Muncipinto, C.D. Altomare, A. Nurisso, P.A. Carrupt, A. Carotti, Structure-Based Design and Optimization of Multitarget-Directed 2H−Chromen-2-one Derivatives as Potent Inhibitors of Monoamine Oxidase B and Cholinesterases, J. Med. Chem. 58 (2015) 5561−5578.

[16] J. Grimsby, N.C. Lan, R. Neve, K. Chen, J.C. Shih, Tissue Distribution of Human Monoamine Oxidase-A and Oxidase-B Messenger-RNA. J. Neurochem. 55 (1990) 1166−1169.

[17] M.B.H. Youdim, D. Edmondson, K.F. Tipton, The therapeutic potential of monoamine oxidase inhibitors, Nat. Rev. Neurosci. 7 (2006) 295-309.

[18] C. J. Fowler, S.B. Ross, Selective Inhibitors of Monoamine Oxidase A and B: Biochemical, Pharmacological, and Clinical Properties. Med. Res. Rev. 4 (1984) 323 −358.

[19] L. Pisani, M. Catto, F. Leonetti, O. Nicolotti, A. Stefanachi, F. Campagna, A. Carotti, Targeting Monoamine Oxidases with Multipotent Ligands: An Emerging Strategy in the Search of New Drugs Against Neurodegenerative Diseases, Curr. Med. Chem. 18 (2011) 4568−4587.

[20] C. Lu, Q. Zhou, J. Yan, Z. Du, L. Huang, X. Li, A novel series of tacrineeselegiline hybrids with cholinesterase and monoamine oxidase inhibition activities for the treatment of Alzheimer's disease, Eur. J. Med. Chem. 62 (2013) 745-753.

[21] D. Salat, E. Tolosa, Levodopa in the Treatment of Parkinson's Disease: Current

Status and New Developments. J. Parkinson's Dis. 2013, 3, 255−269.

[22] Q. He, J. Liu, J.S. Lan, J. Ding, Y. Sun, Y. Fang, N. Jiang, Z. Yang, L. Sun, Y. Jin, S.S. Xie, Coumarin-dithiocarbamate hybrids as novel multitarget AChE and MAO-B inhibitors against Alzheimer's disease: Design, synthesis and biological evaluation, Bioorganic Chemistry 81 (2018) 512–528.

[23] M.D. Mertens, S. Hinz, C.E. Müller, M. Gütschow, Alkynyl–coumarinyl ethers as MAO-B inhibitors, Bioorg. Med. Chem. 22 (2014) 1916-1928.

[24] Z. Sang, K. Wang, J. Shi, X. Cheng, G. Zhu, R. Wei, Q. Ma, L. Yu, Y. Zhao, Z. Tan, W. Liu, Apigenin-rivastigmine hybrids as multi-target-directed liagnds for the treatment of Alzheime r' s disease, Eur. J. Med. Chem. 187 (2020) 111958-111979.

[25] Jiang N., Li S.Y., Xie S.S., Yao H.Q., Sun H.B., Wang X.B., Kong L.Y., $FeCl_3$ and ether mediated direct intramolecular acylation of esters and their application in efficient preparation of xanthone and chromone derivatives. Rsc. Adv. 4 (2014) 63632–63641.

[26] R.F. Sowade, T.R. Jahn, Seed-induced acceleration of amyloid-β mediated neurotoxicity in vivo, Nat. Commun. 8 (2017) 512.

[27] S. Chakrabarti, M. Sinha, I.G. Thakurta, P. Banerjee, M. Chattopadhyay, Oxidative Stress and Amyloid Beta Toxicity in Alzheimer's Disease: Intervention in a Complex Relationship by Antioxidants, Curr. Med. Chem. 20 (2013) 4648−4664.

[28] J. Wang, P. Cai, X.L. Yang, F. Li, J.J. Wu, L.Y. kong, X.B. Wang, Novel cinnamamide-dibenzylamine hybrids: Potent neurogenic agents with antioxidant, cholinergic, and neuroprotective properties as innovative drugs for Alzheimer's disease, Eur. J. Med. Chem. 139 (2017) 68-83.

[29] B. Kumar, V. Kumar, V. Prashar, S. Saini, A.R. Dwivedi, B. Bajaj, D. Mehta, J. Parkash, V. Kumar, Dipropargyl substituted diphenyl pyrimidines as dual inhibitors of monoam ine oxidase and acetylcholin esterase, Eur. J. Med. Chem. 177 (2019) 221-234.

[30] S.A. Eisen, D. K. Miller, R.S. Woodward, E. Spitznagel, T.R. Przybeck, The Effect of Prescribed Daily Dose Frequency on Patient Medication Compliance. Arch. Intern. Med. 1990, 150 (9), 1881−1884.

[31] F. Benazzi, Severe Anticholinergic Side Effects with Venlafaxine-Fluoxetine Combination, Can. J. Psychiat. 1997, 42 (9), 980−981

[32] J. Lo¨tsch, G. Geisslinger, Low-Dose Drug Combinations Along Molecular Pathways Could Maximize Therapeutic Effectiveness While Minimizing Collateral Adverse Effects, Drug Discovery Today 2011, 16 (23), 1001−1006.

[33] A. Anighoro, J. Bajorath, G. Rastelli, Polypharmacology: Challenges and Opportunities in Drug Discovery, J. Med. Chem. 2014, 57 (19), 7874−7887.

[34] A. Cavalli, M.L. Bolognesi, A. Minarini, M. Rosini, V. Tumiatti, M. Recanatini, C. Melchiorre, Multi-target-Directed Ligands To Combat Neurodegenerative Diseases, J. Med. Chem. 2008, 51(3): 349-374.

[35] J. Zhou, X. Jiang, S. He, H. Jiang, F. Feng, W. Liu, W. Qu, H. Sun, Rational Design of Multitarget-Directed Ligands: Strategies and Emerging Paradigms, J. Med. Chem. 2019, 62(20):8881-8914.

[36] J.B. Sun, N. Jiang, M.Y. Lv, P. Wang, F.G. Xu, J.Y. Liang, W. Qu, Limonoids from the root bark of Dictamnus angustifolius: potent neuroprotective agent with biometal chelation, halting copper redox cycling properties. Rsc. Adv. 5 (2015) 24750-24757.

[37] N. Jiang, Q.C. Huang, J. Liu, N.S. Liang, Q. Li, Q.H. Li, S.S. Xie, Design, Synthesis and Biological Evaluation of New Coumarin-dithiocarbamate Hybrids as Multifunctional Agents for the treatment of Alzheimer's Disease, Eur. J. Med. Chem. 146 (2018) 287-298.

[38] N. Jiang, J. Ding, J. Liu, X. Sun, Z. Zhang, Z. Mo, X. Li, H. Yin, W.Z. Tang, S.S. Xie, Novel chromanone-dithiocarbamate hybrids as multifunctional AChE inhibitors with β-amyloid anti-aggregation properties for the treatment of Alzheimer's disease, Bioorganic Chemistry 89 (2019) 103027-103038.

[39] H. Yin, N. Jiang, C. Guo, J.M. Gao, A new bergamotane sesquiterpenoid from the rhizomes of Amomum villosum var. xanthioides Natural Product Research (2019) doi.org/10.1080/14786419.2019.1633649.

[40] L. Di, E.H. Kerns, G.T. Carter, Strategies to assess blood–brain barrier penetration, Expert Opin. Drug Discov. (2008) 3(6):677-687.

[41] V. Mangas-Sanjuan, M. González-Alvarez, I. Gonzalez-Alvarez, M. Bermejo, Drug penetration across the blood–brain barrier: an overview, Therapeutic Delivery (2010) 1(4), 535–562.

[42] D.E. Clark, In silico prediction of blood–brain barrier permeation, Drug Discovery today, 8 (2003) 927-933.

[43] M. Lobell, L. Molnar, G.M. Keseru, Recent Advances in the Prediction of Blood – Brain Partitioning from Molecular Structure, Journal of Pharmaceutical Science, 92 (2003) 360-370.

[44] A. Holt, D.F. Sharman, G.B. Baker, M.M. Palcie, A Continuous Spectrophotometric Assay for Monoamine Oxidase and Related Enzymes in Tissue Homogenates, Anal. Biochem. 244 (1997) 384-392.

[45] C. Zhang, K. Yang, S. Yu, J. Su, S. Yuan, J. Han, Y. Chen, J. Gu, T. Zhou, R. Bai, Y. Xie, Design, synthesis and biological evaluation of hydroxypyridinone-coumarin hybrids as multimodal monoamine oxidase B inhibitors and iron chelates against Alzheimer's disease, Eur. J. Med. Chem. 180 (2019) 367-382.

[46] N.T. Tzvetkov, H.G. Stammler, S. Hristova, A.G. Atanasov, L. Antonov, (Pyrrolo-pyridin-5-yl)benzamides: BBB permeable monoamine oxidase B inhibitors with neuroprotective effect on cortical neurons, Eur. J. Med. Chem. 162 (2019) 793-809.

[47] D. Knez, N. Colettis, L.G. Iacovino, M. Sova, A. Pišlar, J. Konc, S. Lešnik, J. Higgs, F. Kamecki, I. Mangialavori, A. Dolšak, S. Žakelj, J. Trontelj, J. Kos, C. Binda, M. Marder, S. Gobec, Stereoselective Activity of 1-Propargyl-4-styrylpiperidine-like Analogues That Can Discriminate between Monoamine Oxidase Isoforms A and B, J. Med. Chem. 2020, 63(3):1361-1387.

[48] J. Reis, F. Cagide, D. Chavarria, T. Silva, C. Fernandes, A. Gaspar, E. Uriarte, F. Remiao, S. Alcaro, F. Ortuso, F. Borges, Discovery of New Chemical Entities for Old Targets: Insights on the Lead Optimization of Chromone-Based Monoamine Oxidase B (MAOB) Inhibitors, J. Med. Chem. 2016, 59, 5879−5893

[49] Y.W. Tang, C.J. Shi, H.L. Yang, P. Cai, Q.H. Liu, X.L. Yang, L.Y. Kong, X.B. Wang, Synthesis and evaluation of isoprenylation-resveratrol dimer derivatives

against Alzheimer's disease. Eur. J. Med. Chem. 163 (2019) 307-319

[50] C. Zhang, K. Yang, S. Yu, J. Su, S. Yuan, J. Han, Y. Chen, J. Gu, T. Zhou, R. Bai, Y. Xie. Design, synthesis and biological evaluation of hydroxypyridinone-coumarin hybrids as multimodal monoamine oxidase B inhibitors and iron chelates against Alzheime r's disease. Eur. J. Med. Chem. 180 (2019) 367-382.

[51] R. Purgatorio, M. Candia, M. Catto, A. Carrieri et al. Investigating 1,2,3,4,5,6-hexahydroazepino[4,3-b]indole as scaffold of butyrylcholinesterase-selective inhibitors with additional neuroprotective activities for Alzheimer's disease. Eur. J. Med. Chem. 177 (2019) 414-424.

[52] W. Huang, M. Liang, Q. Li, X. Zheng, C. Zhang, Q. Wang, L. Tang, Z. Zhang, B. Wang, Z. Shen, Development of the " hidden" multifunctional agents for Alzheimer's disease, Eur. J. Med. Chem. 177 (2019) 247-258.

[53] L. Jalili-Baleh, H. Forootanfar, Tuba.Tüü. Küçükkılınç, H. Nadri, Z. Abdolahi, A. Ameri, M. Jafari, B. Ayazgok, M. Baeeri, M. Rahimifard, S.N. Abbas Bukhari, M. Abdollahi, M.R. Ganjali, S. Emami, M. Khoobi, A. Foroumadi, Design, synthesis and evaluation of novel multi-targetdirected ligands for treatment of Alzheimer's disease based on coumarin and lipoic acid scaffolds, Eur. J. Med. Chem. 152 (2018) 600-614.

[54] L. Di, E.H. Kerns, K. Fan, O.J. McConnell, G.T. Carter, High throughput artificial membrane permeability assay for blood-brain barrier, Eur. J. Med. Chem. 38 (2003) 223–232.

[55] X. Li, H. Wang, Z. Lu, X. Zheng, W. Ni, J. Zhu, Y. Fu, F. Lian, N. Zhang, J. Li, H. Zhang, F. Mao, Development of multifunctional pyrimidinylthiourea derivatives as potential anti-Alzheimer agents, J. Med. Chem. 59 (2016) 8326–8344.

[56] H. Zheng, S. Gal, L.M. Weiner, O. Bar-Am, A. Warshawsky, M. Fridkin, M.B.H. Youdim, J. Neurochem. 95 (2005) 68-78.

[57] M. Yanez, N. Fraiz, E. Cano, F. Orallo, Inhibitory effects of cis- and trans-resveratrol on noradrenaline and 5-hydroxytryptamine uptake and on monoamine oxidase activity, Biochem. Biophys. Res. Commun. 344 (2006) 688–695.

[58] M.J. Matos, C. Teran, Y. Perez-Castillo, E. Uriarte, L. Santana, D. Vina, Synthesis and study of a series of 3-arylcoumarins as potent and selective monoamine

oxidase B inhibitors, J. Med. Chem. 54 (2011) 7127–7137.

[59] L.J. Legoabe, A. Petzer, J.P. Petzer, Selected C7-substituted chromone derivatives as monoamine oxidase inhibitors, Bioorg. Chem. 45 (2012) 1–11.

[60] Z.R. Wang, Y.L. Wang, B. Wang, W.R. Li, L. Huang, X.S. Li, Design, Synthesis, and Evaluation of Orally Available Clioquinol-Moracin M Hybrids as Multitarget-Directed Ligands for Cognitive Improvement in a Rat Model of Neurodegeneration in Alzheimer's Disease, J. Med. Chem. 58 (2015) 8616-8637.

[61] X. Li, H. Wang, Z. Lu, X. Zheng, W. Ni, J. Zhu, Y. Fu, F. Lian, N. Zhang, J. Li, H. Zhang, F. Mao, Development of multifunctional pyrimidinylthiourea derivatives as potential anti-Alzheimer agents, J. Med. Chem. 59 (2016) 8326 –8344.

[62] Q. Li, L. Meng, S. Zhou, X. Deng, N. Wang, Y. Ji, Y. Peng, J. Xing, G. Yao, Rapid generation of novel ben zoic acidebased xanthine derivatives as highly potent, selective and long acting DPP-4 inhibitors: Scaffoldhopping and prodrug study, Eur. J. Med. Chem. 180 (2019) 509-523.

Highlights

- Twenty rasagiline-clorgyline hybrids were designed and synthesized.
- All compounds were highly selective and potent *h*MAO-B inhibitors.
- **6j** exhibited low nanomolar inhibition for MAO-B and good inhibition for $A\beta_{1-42}$ aggregation.
- **6j** showed neuroprotective effects and could penetrate the BBB.
- **6j** had good pharmacokinetic characteristics after intravenous and oral administrations.

Design, synthesis and biological evaluation of rasagiline-clorgyline hybrids as novel dual inhibitors of monoamine oxidase-B and amyloid-β aggregation against Alzheimer's disease

Sai-Sai Xie[#a,c], Jing Liu[#a,d], Chunli Tang[a], Chengyun Pang[a], Qing Li[a], Yuelian Qin[a], Xiaojie Nong[a], Zhipeng Zhang[c], Jie Guo[c], Maojun Cheng[c], Weizhong Tang[b], NingSheng Liang[a,*], Neng Jiang[a,*]

[a]Department of Pharmacy, [b]Department of Gastrointestinal Surgery, Affiated Tumor Hospital of Guangxi Medical University, Nanning, PR China

[c]National Pharmaceutical Engineering Center for Solid Preparation in Chinese Herbal Medicine, [d]School of Pharmacy, Jiangxi University of Traditional Chinese Medicine, Nanchang, PR China

Notes

The authors declare no competing financial interest.